Physical-biological oceanographic coupling influencing phytoplankton and primary production in the South China Sea

X. Ning[1]

Key Labs of Ocean Dynamic Processes and Satellite Oceanography and Submarine Sciences, State Oceanic Administration, Hangzhou, Zhejiang, China

F. Chai and H. Xue

School of Marine Sciences, University of Maine, Orono, Maine, USA

Y. Cai, C. Liu, and J. Shi

Second Institute of Oceanography, State Oceanic Administration, Hangzhou, Zhejiang, China

Received 4 March 2004; revised 1 June 2004; accepted 1 July 2004; published 13 October 2004.

[1] Two cruises were carried out in the summer and winter of 1998 to study coupled physical-chemical-biological processes in the South China Sea and their effects on phytoplankton stock and production. The results clearly show that the seasonal distributions of phytoplankton were closely related to the coupled processes driven by the East Asian Monsoon. Summer southwesterly monsoon induced upwelling along the China and Vietnam coasts. Several mesoscale cyclonic cold eddies and anticyclonic warm pools were identified in both seasons. In the summer, the upwelling and cold eddies, both associated with rich nutrients, low dissolved oxygen (DO), high chlorophyll *a* (Chl *a*) and primary production (PP), were found in the areas off the coast of central Vietnam, southeast of Hainan Island and north of the Sunda shelf, whereas in the winter they form a cold trough over the deep basin aligning from southwest to northeast. The warm pools with poor nutrients, high DO, low Chl *a*, and PP were found in the areas southeast of Vietnam, east of Hainan, and west of Luzon during the summer, and a northwestward warm jet from the Sulu Sea with properties similar to the warm pools was encountered during the winter. The phytoplankton stock and primary production were lower in summer due to nutrient depletion near the surface, particularly PO_4. This phosphorus depletion resulted in phytoplankton species succession from diatoms to dinoflagellates and cyanophytes. A strong subsurface Chl *a* maximum, dominated by photosynthetic picoplankton, was found to contribute significantly to phytoplankton stocks and production. *INDEX TERMS:* 4223 Oceanography: General: Descriptive and regional oceanography; 4853 Oceanography: Biological and Chemical: Photosynthesis; 4855 Oceanography: Biological and Chemical: Plankton; 4845 Oceanography: Biological and Chemical: Nutrients and nutrient cycling; *KEYWORDS:* South China Sea, phytoplankton and nutrients, primary production, physical-biological coupling processes

Citation: Ning, X., F. Chai, H. Xue, Y. Cai, C. Liu, and J. Shi (2004), Physical-biological oceanographic coupling influencing phytoplankton and primary production in the South China Sea, *J. Geophys. Res.*, *109*, C10005, doi:10.1029/2004JC002365.

1. Introduction

[2] In large areas of the tropical Pacific Ocean, the standing stock and production of phytoplankton are very low, although there is ample light penetration to drive photosynthesis. This paucity of biomass and production is the result of a euphotic zone that is impoverished with respect to essential macro-nutrients and trace metals, due to the permanent stratification of the water column. Enhancement of biomass and production of phytoplankton occurs episodically when mesoscale physical phenomena increase the concentration of nutrients in the euphotic zone. Monsoon-driven baroclinic eddies are one of the most common mesoscale features in the tropical and subtropical Pacific Ocean [*Falkowski et al.*, 1991; *Olaizola et al.*, 1993; *McGillicuddy et al.*, 1998; *Seki et al.*, 2001], including the South China Sea (SCS) [*Chai et al.*, 2001a; *Xu et al.*, 2001]. Baroclinic instability leads to the formation of cyclonic eddies with a raised thermocline and anticyclonic eddies with a depressed thermocline. When the nutricline and thermocline are coincident, enhanced phytoplankton production is expected in cyclonic eddies

[1]Also at Second Institute of Oceanography, State Oceanic Administration, Hangzhou, Zhejiang, China.

0148-0227/04/2004JC002365$09.00

[*Williams and Follows*, 2003]. Recent studies demonstrated that the effects of coupling between physical and biological processes on phytoplankton biomass and production, for example, the causative link of ''monsoon-circulation-nutrients-phytoplankton,'' are substantial for understanding plankton dynamics [*Allen et al.*, 1996; *Ning and Liu*, 1988; *Gong et al.*, 2000; *Liu et al.*, 2002].

[3] Most oceanographic studies for the SCS have focused on physical oceanographic processes and circulation modeling [*Rong*, 1994; *Chao et al.*, 1996; *Metzger and Hurlburt*, 1996; *Chu et al.*, 1997; *Fang et al.*, 1998; *Guan*, 1998; *Su et al.*, 1999; *Chai et al.*, 2001a, 2001b, 2001c; *Xu et al.*, 2001; *Xue et al.*, 2001a, 2001b, 2004], and a few studies on chemical oceanography [*Gong et al.*, 1992; *Han et al.*, 1998; *Chen et al.*, 2001; *Cai et al.*, 2002]. Regarding the biological oceanography in the SCS, even general descriptions on phytoplankton biomass, primary production, and the governing environmental factors are sparse. A few studies were conducted in limited areas off Xisha and Zhongsha Islands [*Liu and Liu*, 1984], Nansha Islands [*Huang*, 1988, 1991; *Huang and Chen*, 1997], in the central basin [*Chen et al.*, 1989], Gulf of Beibu [*Liu et al.*, 1998], Sulu Sea [*San Diego-McGlone et al.*, 1999], and a few transects completed by *Hung and Tsai* [1972] and *Takahashi and Hori* [1984]. Combining model results and limited observations, *Liu et al.* [2002] examined the seasonal cycle of phytoplankton and productivity in the SCS. A large-scale biological oceanographic survey of the greater SCS has not been reported, and there are no size-fractionated measurements of phytoplankton stock and production in this sea area.

[4] The present study is a part of a multidisciplinary project, which offered an excellent opportunity to understand the following: (1) How do physical oceanographic processes govern nutrient distribution? (2) What is the role of physical oceanographic processes in maintaining and modulating biological productivity? (3) How are the spatial and temporal variations of phytoplankton biomass and production related to physical and chemical environmental factors? (4) What is the relationship between monsoonal forcing, circulation and biological production and what are the contributions of different sized plankton to standing stock and production of phytoplankton communities in the SCS?

2. Study Area

[5] The South China Sea (SCS) (Figure 1) is the largest marginal sea in Southeast Asia with an area of about 3.5 millions km^2. It is bounded by the China continent on the north and northwest sides, Vietnam and Gulf of Thailand on the west and the southwest sides, Sunda Shelf and Borneo on the south side, and Taiwan and Philippine on the east side. The deep basin with a maximum depth reaching 4700 m in the center of the SCS is bordered by the northern and southern continental shelves which are broad and shallow with depths of <200 m, while on the east and west sides it is bordered by narrow shelves or steep slopes. The SCS is connected to the open ocean through many passages, but there is only one major channel, the Luzon Strait (also known as the Bashi Strait), where a deep sill (>2000 m [*U.S. Naval Oceanographic Office*, 1969]), allows effective water exchange with the western Pacific. Runoff from several large rivers, including the Pearl and Mekong Rivers, carries a large quantity of fresh water and dissolved nutrients into the SCS (Figure 1).

[6] The meteorological forcing over the SCS is dominated by the East Asian Monsoon [*Sadler et al.*, 1985]. In January, an atmospheric high pressure center is situated over the northwest of China and the corresponding Aleutian low is situated over the northern Pacific, resulting in the northerly monsoon; while in July, the atmospheric high pressure is located over the northwestern Pacific and the low pressure is located over Tibet, resulting in the southerly monsoon [*Tao*, 1978]. The southwest monsoon prevails from June to August (summer), while the northeast monsoon prevails from November to February (winter). Spring and autumn are transitional seasons when the wind direction is more variable. The latitudinal gradients of the sea surface temperature (SST) across the basin are the largest during winter (from <20°C in the northern coast to >29°C in the southern end), but more uniform during summer (from 28°C in the northern coast to 31.5°C in the southern end).

[7] The upper ocean circulation of the SCS follows closely the alternating monsoons [*Wyrtki*, 1961]. The winter monsoon drives a large-scale cyclonic gyre over the entire deep basin with a strong southward current along the coast of Vietnam [*Wyrtki*, 1961; *Shaw and Chao*, 1994]. Along the northern boundary of the basin, Kuroshio water with warm, saline and oligotrophic properties intrudes through the Luzon Strait to become the deep-water mass of the SCS [*Nitani*, 1972]. *Shaw* [1991] also showed that the surface Kuroshio water from the Philippine Sea intrudes into the SCS and flows westward along the continental margin of China. Furthermore, during the northeast monsoon, the coastal water of the East China Sea flows southwestward through the Taiwan Strait into the SCS [*Fang et al.*, 1998]. On the contrary, the summer southwest monsoon forces a large-scale anti-cyclonic circulation, which bifurcates off the central coast of Vietnam. The northeast flowing branch encloses an anti-cyclonic gyre in the southern basin, while next to the coast the flow continues northward. The latter becomes part of the eastward Guangdong Coastal Current along the continental shelf of China, which eventually flows into the East China Sea through the Taiwan Strait. The southwesterly winds also induce seaward Ekman transport and coastal upwelling. The deep water upwells and mixes with the surface waters to form the SCS intermediate water, which flows out of the SCS through the Luzon Strait [*Gong et al.*, 1992]. Embedded in the basin-scale circulation gyres are localized mesoscale features: off the coast of Vietnam during summer, and to the northwest of Luzon and north of the Sunda Shelf during winter [*Chao et al.*, 1996; *Shaw et al.*, 1996; *Xu et al.*, 2001].

3. Materials and Methods

[8] The area that was surveyed is located between 6°00′N and 23°00′N in latitude and 108°00′E and 120°00′E in longitude. Two cruises were conducted during the southwest monsoon (summer: 12 June to 6 July 1998) and northeast monsoon (winter: 28 November to 28 December 1998). An array of 61 stations (see Figure 1) was sampled. Seawater samples were taken with a rosette of Niskin

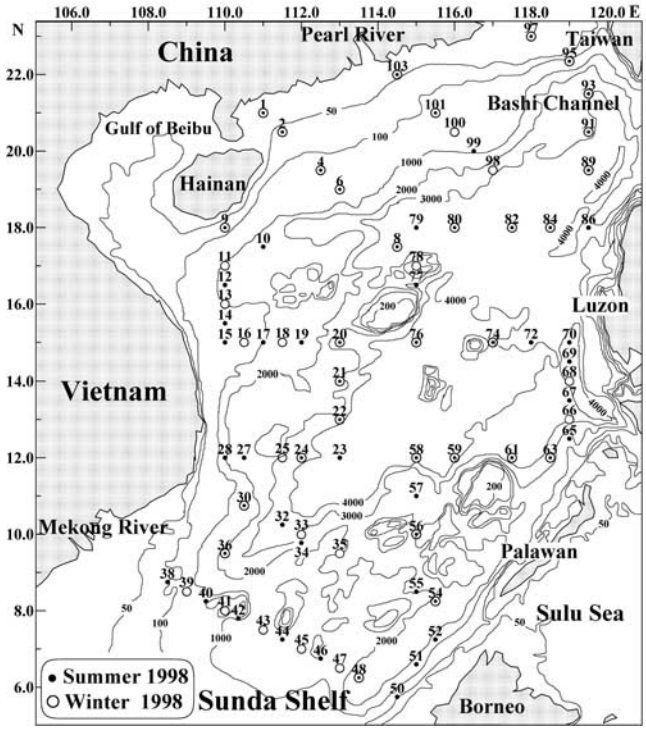

Figure 1. Sampling stations of the 1998 SCS survey cruise. Solid circles, summer cruise; open circles, winter cruise. Contours represent the bottom topography with marked water depths.

bottles attached to a CTD (Conductivity-Temperature-Depth system, Niel Brown Mark III) probe frame. Water samples for chlorophyll (Chl) determinations were taken at 0, 10, 25, 50, 75, 100, and 150 m. At the beginning of every cruise leg and subsequently every 4 days, the water samplers (10-L Niskin bottles) were inspected for evidence of biological and organic films on the interior walls, valves and caps. If found, biological films were removed using brushes, scouring agents and detergent solutions without any nutrients. Finally, the water samplers were rinsed using distilled water several times. During sampling, we made sure that the sample was free from ship discharge (garbage, sewage, bilge, etc.).

[9] Photosynthetic rates were determined at selected stations (Stations 004, 012, 021, 024, 034, 044, 056, 061, 067, 079, 091, and 101 in summer and 008, 016, 021, 041, 048, 061, 068, 078, 084, and 103 in winter). Sampling depths corresponded to light levels of 100, 50, 32.5, 10, 3, and 1% of the surface irradiance. At stations where primary productivity was measured, profiles of downward irradiance (PAR) were obtained by using a LI-COR 1000 data logger equipped with a LI-193SB underwater 4π spherical quantum sensor.

[10] Nutrients (nitrate, phosphate, and silicate) were analyzed by standard spectrophotometric methods, and dissolved oxygen (DO) was analyzed by Winkler procedure [*Strickland and Parsons*, 1972]. The detection limits of the three nutrients were 0.05, 0.03, and 0.1 μmol dm^{-3}, respectively, and that of DO was 0.5 μmol dm^{-3}. Photosynthetic pigments (Chl *a* and phaeopigments) were measured by the acetone extraction fluorescence method [*Holm-Hansen et al.*, 1965] using 250 mL of seawater samples. Since the fluorometric procedure for chlorophyll *a* determination can suffer from interference from chlorophyll b or divinyl chlorophyll b-containing *Prochlorococcus* [*Goericke and Repeta*, 1993], which is usually abundant in oligotrophic tropical waters, we often used spectrophotometry to calibrate the results obtained by using fluorometry.

[11] Photosynthetic rates and primary productivity were measured by using the isotopic (^{14}C) tracer method established by *Steemann Nielsen* [1952] and improved by *Evans et al.* [1987] and *Ning et al.* [1988]. Water samples taken from each light level were used to fill two light bottles and one dark bottle of 250 mL. To each bottle, 10 μCi of $NaH^{14}CO_3$ was added and placed in an incubator on the ship's deck, and incubated for about 6 hours (usually from noon to sunset). Sieves with a gradient of neutral light density were used to achieve a range of incubation light intensities that corresponded to the original sampling depths. A seawater circulation system maintained the in situ temperature. After incubation, the water samples were filtered; the filters were fumed over concentrated HCl, dried, and preserved in the dark. Counts were made by using a liquid scintillation counter (Beckman LS 5801).

[12] Before dispensing, all water samples were prefiltered through a 280-μm mesh to remove larger zooplankton. Water samples for the determinations of size-fractionated chlorophyll and photosynthetic rates were filtered through 20-μm mesh (for retention of net-plankton), a Nuclepore filter of 2.0 μm in pore size (for retention of nano- and net-plankton), and a Whatman GF/F filter (for retention of pico-, nano- and net-plankton) after incubation. After analyzing the content of each filter, the three fractions could be easily calculated. Phytoplankton species identification and cell counts were made from 500 mL of seawater samples fixed in neutral formalin [*Sournia*, 1978] using an inverted microscope.

4. Results

4.1. Environmental Features

[13] Only a brief description of major oceanographic features in the SCS, especially distributions of physical and chemical parameters relevant to the observed phytoplankton stock and production, is provided. Details about the features are given by *Chai et al.* [2001a, 2001b, 2001c] and *Xu et al.* [2001]. Furthermore, the observed results at the depth of 75 m are presented. This depth is chosen since this layer, usually just below the thermocline and near the bottom of the euphotic zone, represents a mixture of the SCS Surface Water and the SCS Subsurface Water [*Liu et al.*, 2001], which is relatively stable and still reflects primarily the influence of monsoon forcing on plankton dynamics. Furthermore, in order to better understand the physical-biological coupling associated with mesoscale features, vertical distributions of phytoplankton, and the related environmental parameters on the transects across some typical mesoscale eddies are also provided in section 5.

4.1.1. Hydrological Conditions

[14] In general, the observed hydrographic features (see Figure 2) agree with the summertime (wintertime) basin-scale anti-cyclonic (cyclonic) circulation such that the temperature was high and the salinity was low in the central

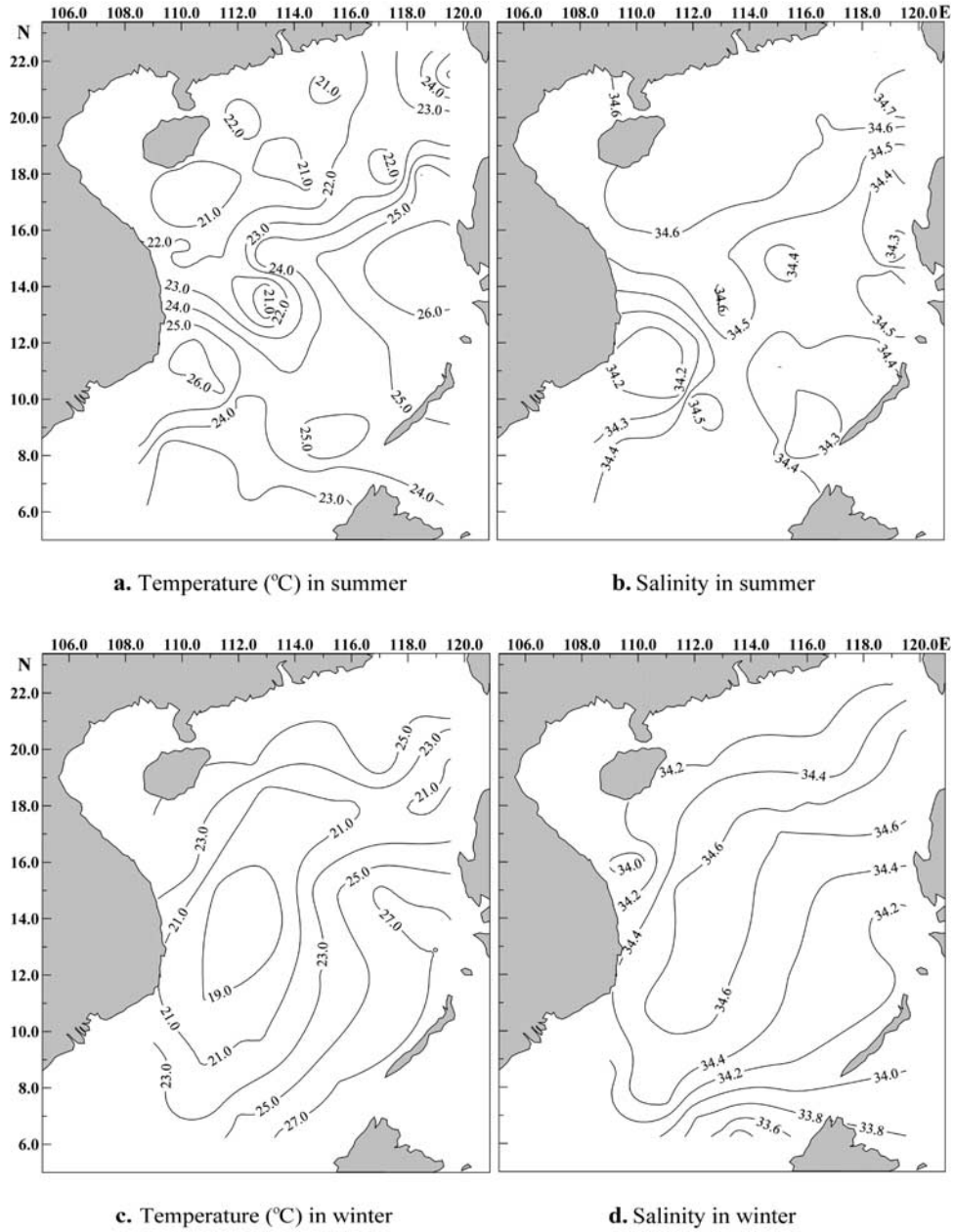

Figure 2. Seawater temperature (°C) and salinity in the SCS at 75 m, 1998. (a) Temperature in summer, (b) salinity in summer, (c) temperature in winter, and (d) salinity in winter.

basin in the summer and vice versa in the winter. However, the basin-scale circulation was distorted considerably due to mesoscale eddies, especially during the summer (Figures 2a and 2b).

[15] In summer, the water temperature ranged from 20.12°C (at Station 012) to 27.51°C (at Station 072) with a mean of 23.71°C, and the salinity ranged from 34.09 (at Station 027) to 34.86 (at Station 091) with a mean of 34.47 (Table 1). The waters with low temperature (<22°C) and high salinity (>34.6) occupied the northern and northwestern continental shelf and slope (Figures 2a and 2b). The low temperature signal appeared to be patchy, with the lowest temperature encountered in the area southeast of Hainan Island (Figure 2a). In addition, two other areas of low temperature and high salinity were found east of Vietnam and north of the Sunda Shelf from 108°E to 116°E where T < 23°C and S > 34.4. The former, also detected from satellite observations [*Kuo et al.*, 2000], was associated with a cyclonic eddy centered at 13°N and 113°E, and the latter probably resulted from the upward motion on the slope induced by the basin-scale anticyclonic gyre. The areas with higher temperature (>25°C) and lower salinity (<34.4) were found in the eastern half of the basin along the coasts of Luzon and Palawan, except for a small area northwest of the Mindoro Strait where the salinity is higher than 34.5. In addition, the area off the coast of southeast Vietnam was also occupied by a high temperature and low salinity water mass, corresponding to an anticyclonic eddy. The mesoscale features discussed above are summarized in Table 2a. Similar eddy dipoles east of Vietnam with an anticyclonic

Table 1. Mean ± SD and Range (in Parentheses) of Physical, Chemical, and Biological Parameters at the Surface and 75 m in the SCS in 1998

	Summer		Winter	
Parameter	Surface (n = 61)	75 m (n = 56)	Surface (n = 49)	75 m (n = 41)
Temperature, °C	30.37 ± 0.64 (28.50 ~ 31.64)	23.7 ± 2.09 (20.12 ~ 27.51)	26.65 ± 2.30 (15.64 ~ 29.28)	23.09 ± 3.18 (15.31 ~ 29.51)
Salinity	33.46 ± 1.39 (24.52 ~ 34.63)	34.47 ± 0.16 (34.09 ~ 34.86)	32.54 ± 1.88 (26.01 ~ 34.70)	34.34 ± 0.36 (33.29 ~ 34.70)
NO_3, μmol dm^{-3}	0.50 ± 1.58 (0.00 ~ 12.3)	1.27 ± 1.95 (0.00 ~ 7.54)	0.89 ± 1.62 (0.00 ~ 6.37)	4.08 ± 4.41 (0.01 ~ 13.90)
NO_2, μmol dm^{-3}	0.05 ± 0.13 (0.00 ~ 0.97)	0.08 ± 0.10 (0.00 ~ 0.48)	0.19 ± 0.32 (0.00 ~ 1.20)	0.15 ± 0.14 (0.01 ~ 0.47)
NH_4, μmol dm^{-3}	1.58 ± 1.17 (0.37 ~ 7.35)	1.16 ± 0.49 (0.31 ~ 2.10)	1.50 ± 0.47 (0.46 ~ 2.78)	1.31 ± 0.40 (0.52 ~ 2.29)
PO_4, μmol dm^{-3}	0.05 ± 0.04 (0.00 ~ 0.23)	0.13 ± 0.13 (0.00 ~ 0.53)	0.38 ± 0.37 (0.05 ~ 1.87)	0.51 ± 0.47 (0.06 ~ 2.36)
SiO_3, μmol dm^{-3}	1.22 ± 0.67 (0.22 ~ 2.83)	2.96 ± 2.07 (0.29 ~ 9.56)	2.85 ± 5.73 (0.00 ~ 22.00)	4.95 ± 4.35 (0.00 ~ 20.00)
DO, μmol dm^{-3}	402.1 ± 16.4 (340.0 ~ 456.9)	395.8 ± 42.1 (244.5 ~ 453.3)	417.5 ± 41.0 (207.20 ~ 500.10)	353.3 ± 49.5 (256.3 ~ 435.9)
Chl *a*, μg dm^{-3}	0.11 ± 0.07 (0.02 ~ 0.41)	0.26 ± 0.16 (0.01 ~ 0.88)	0.29 ± 0.34 (0.01 ~ 1.87)	0.36 ± 0.40 (0.02 ~ 1.95)
Phytopl. abund. ($\times 10^3$ cell dm^{-3})	0.83 ± 3.22 (0.09 ~ 24.60)		8.46 ± 14.07 (0.26 ~ 65.62)	
PPP, mgC m^{-3} h^{-1}	1.31 ± 0.85 (n = 12) (0.31 ~ 2.56)		1.35 ± 1.32 (n = 10) (0.19 ~ 3.75)	0.92 ± 0.18 (n = 8) (0.68 ~ 1.22)
PP,[a] mgC m^{-2} d^{-1}	389.8 ± 342.5 (n = 12) (94.5 ~ 1305.8)		546.0 ± 409.4 (n = 10) (145.8 ~ 1605.5)	

[a]Daily integrated primary production within euphotic zone.

to the south coupled with a cyclonic eddy to the north (or northeast, in this case) were also found in the model results of *Xue et al.* [2004].

[16] In winter, the temperature ranged from 15.31°C (at Station 082) to 29.51°C (at Station 066) with a mean of 23.09°C; the salinity ranged from 33.29 (at Station 048) to 34.70 (at Station 084) with a mean of 34.34 (Table 1). Waters of high temperature (>25.0°C) and low salinity (<34.2) were encountered in both the northern and northwestern regions along the coasts of China and northern Vietnam and the southern and southeastern regions along the coasts of Borneo and Palawan. The latter has a tongue-like feature extending northwestward from the Mindoro Strait into the deep basin of the SCS (Figures 2c and 2d). Bounded by the high temperature and low salinity waters to the north and south was a large area with low temperature (<23.0°C) and high salinity (>34.4). The area covered the central basin eastward to the Luzon Strait from 7°N to 19°N and from 109°E to 120°E, roughly inside the 1000-m isobath. Note that the nose-like distribution of low temperature and high salinity near the southern tip of this area was consistent with the notion of a small, enclosed cyclonic eddy there [*Xue et al.*, 2004]. Hence there should be upward vertical velocity in the center of this cyclonic eddy. Hydrographic characteristics of the wintertime mesoscale feature are summarized in Table 2b.

Table 2a. Mean (±SD) of Physical, Chemical, and Biological Parameters in the Major Mesoscale Eddies in the SCS at 75 m in Summer 1998

Parameters Mesoscale Eddy	Temperature, °C	Salinity	NO_3, μmol dm^{-3}	PO_4, μmol dm^{-3}	SiO_3, μmol dm^{-3}	DO, μmol dm^{-3}	Chl *a*, μg dm^{-3}
Cold eddy							
Southeast of Hainan Island	20.53	34.65	5.44	0.23	5.9	371	0.58
(Stns 9, 12)	(0.58)	(0.05)	(1.81)	(0.20)	(1.41)	(17.3)	(0.01)
Central area off Vietnam	20.57	34.61	4.11	0.32	0.63	364.5	0.40
(Stns 21, 22)	(0.02)	(0)	(4.37)	(0.19)	(0.30)	(56.1)	(0.13)
Warm pool							
East of Hainan Island	21.60	34.66	0.87	0.15	5.65	413.2	0.04
(Stns 4, 6)	(1.29)	(0.04)	(0.75)	(0.08)	(3.32)	(13.9)	(0.02)
Southeast of Vietnam	25.68	34.16	0.39	0.05	1.43	435.7	0.17
(Stns 24, 27, 28, 30)	(0.72)	(0.07)	(0.23)	(0.03)	(0.83)	(12.3)	(0.06)
Basin area of the SCS	25.10	34.39	0.32	0.03	1.12	429.8	0.22
(Stns 58, 59, 61, 74, 76)	(0.90)	(0.05)	(0.29)	(0.02)	(0.62)	(13.74)	(0.04)
Northwest of Luzon Strait (Stn 93)	26.29	34.73	0.17	<0.03	1.6	422.1	0.13
West of Luson (Stn 67)	26.1	34.45	0.44	0.05	1.90	399.8	0.2
Upwelling							
Sunda Shelf break	22.63	34.44	3.08	0.25	3.53	351.6	0.54
(Stns 44, 46, 48)	(0.78)	(0.02)	(2.17)	(0.18)	(2.01)	(40.37)	(0.29)

Table 2b. Mean (±SD) of Physical, Chemical, and Biological Parameters in the Major Mesoscale Eddies in the SCS at 75 m in Winter 1998

Parameters Mesoscale Eddy	Temperature, °C	Salinity	NO_3, μmol dm^{-3}	PO_4, μmol dm^{-3}	SiO_3, μmol dm^{-3}	DO, μmol dm^{-3}	Chl *a*, μg dm^{-3}
Cold eddy							
Northwest of Luson	20.82	34.7	5.49	0.84	4.9	346.6	0.48
(Stns 82, 84)	(0.36)	(0.01)	(0.78)	(0.08)	(1.41)	(2.5)	(0.07)
Central area off Vietnam	18.13	34.66	11.74	0.50	8.84	282.4	0.30
(Stns 18, 20, 21, 22, 24)	(0.44)	(0.02)	(1.30)	(0.26)	(3.24)	(8.8)	(0.17)
Warm jet							
Toward northwest from	25.32	34.36	0.56	0.52	2.00	382.9	0.23
Sulu Sea through Mindolo Strait	(3.76)	(0.23)	(0.65)	(0.41)	(1.15)	(2.1)	(0.12)
(Stns 66, 74, 78)							
Upwelling							
Sunda Shelf break	21.29	34.48	6.48	0.67	7.45	307.3	1.21
(Stns 41, 43)	(0.70)	(0.06)	(0.45)	(0.08)	(1.48)	(20.2)	(0.09)

4.1.2. Chemical Parameters

4.1.2.1. Nutrients (Nitrate, Phosphate, and Silicate)

[17] Nutrient distributions were in general agreement with the hydrographic patterns described above. In summer, high nutrient concentrations ($NO_3 > 2.0$, $PO_4 > 0.2$ and $SiO_3 > 4.0$ μmol dm^{-3}) were found in the cold eddies (CE) southeast of Hainan and east of Vietnam between 12°N and 14°N and between 112°E and 114°E, as well as in the upwelling region north of the Sunda Shelf (see Figures 3a–3c). In contrast, the warm pools (WP) to the east of Hainan, southeast of Vietnam, and west of Luzon were associated with low nutrient concentrations ($NO_3 < 1.0$, $PO_4 < 0.1$ and $SiO_3 < 1.0$ μmol dm^{-3}) except for SiO_3 in the WP to east of Hainan (Tables 1 and 2a).

[18] In winter, nutrient concentrations were generally lower ($NO_3 < 2.0$, $PO_4 < 0.2$, and $SiO_3 < 2.0$ μmol dm^{-3}) in the warm waters on the northern and southern shelves with the exception of higher PO_4 along the coasts of Borneo and Palawan and higher SiO_3 in the vicinity of Dongsha Islands. The central basin where the cyclonic gyre located and the area slightly to the east of the CE on the southern slope were regions of high nutrient concentrations ($NO_3 > 8.0$, $PO_4 > 0.6$ and $SiO_3 > 8.0$ μmol dm^{-3}). The fact that the higher nutrients were found to the east of the CE on the southern slope as defined in hydrography could be the result of horizontal advection by the basin-scale cyclonic circulation in winter. In addition, the cold and saline tongue northwest of the Luzon was also associated with elevated nutrient concentrations with $NO_3 > 4.0$, $PO_4 > 0.6$ and $SiO_3 > 4.0$ μmol dm^{-3} (Figures 4a–4c; Tables 1 and 2b).

[19] To summarize, the cold, cyclonic gyre and eddies were associated with nutrient-rich waters, whereas the warm pools were associated with nutrient-poor waters, which was consistent with generally upward/downward motions inside the cyclonic/anticyclonic features. The basin-wide mean concentration of NO_3, PO_4, and SiO_3 was higher in winter than in summer, and higher at 75 m than at the surface (Table 1).

4.1.2.2. Dissolved Oxygen (DO)

[20] In summer, DO concentrations ranged from 245 (at Station 061) to 453 μmol dm^{-3} (at Station 024) with a mean of 396 μmol dm^{-3} (Table 1). High values of DO (>400 μmol dm^{-3}) were encountered in a large area from the southeast coast of Vietnam extending northeastward to the west of the Luzon Strait, corresponding well with the areas of high temperature and low nutrients. The low values of DO (<375 μmol dm^{-3}) appeared in the areas southeast of Hainan Island, east of central Vietnam, and from the Sunda Shelf to the coast of Borneo, corresponding again with the mesoscale features of low temperature and high nutrients (Figure 3d and Table 2a). However, the lowest DO was found to the north of the Palawan coast centered at 11.5°N and 117.5°E. This area of low DO did not have a counterpart in any other physical or chemical properties.

[21] During winter, DO concentrations ranged from 256 (at Station 045) to 436 μmol dm^{-3} (at Station 004) with a mean of 353 μmol dm^{-3} (Table 1). Again, the high values of DO (>400 μmol dm^{-3}) were encountered in the warm and nutrient-poor waters, and low values of DO (<300 μmol dm^{-3}) were found in the cold and nutrient-rich waters (Figure 4d and Table 2b).

4.2. Standing Stock of Phytoplankton

4.2.1. Chlorophyll *a* (Chl *a*) Concentration

[22] During summer, Chl *a* concentration ranged from 0.01 (at Station 012) to 0.88 mg m^{-3} (at Station 046) with a mean of 0.26 mg m^{-3} (Table 1). High values (>0.3 mg m^{-3}) occurred in several areas: south of Hainan Island, east of Vietnam, and the Sunda Shelf and Slope. These areas coincided generally with the high nutrient concentration found there, except that in the area southeast of Hainan, high nutrient values extended farther to the east compared with the high Chl *a* values. In addition, the intruded Kuroshio water west of the Luzon Strait appeared to have high values of Chl *a* as well. Elsewhere, Chl *a* concentration fell below 0.3 mg m^{-3} and the lower values (<0.2 mg m^{-3}) were encountered in the areas southeast of Vietnam (WP) and east of Hainan (Figure 5a and Table 2a).

[23] During winter, Chl *a* concentrations ranged from 0.02 (at Station 098) to 1.95 mg m^{-3} (at Station 041) with a mean of 0.36 mg m^{-3} (Table 1). There were four areas with Chl *a* concentration >0.4 mg m^{-3}. The highest Chl *a* occurred north of the Sunda Shelf in the area of high nutrient concentrations. A small area in the central basin and an area of about 2° × 2° northwest of Luzon also had Chl *a* > 0.4 mg m^{-3}, corresponding to the high nutrient concentrations in these areas. The area on the northern shelf where the nutrient concentrations were generally low, except for SiO_3, was consistent with the smaller Pearl River Plume in winter. The relatively low Chl *a* concentration (<0.2 mg m^{-3}) appeared in the eastern half of the SCS (Figure 5b and Table 2b).

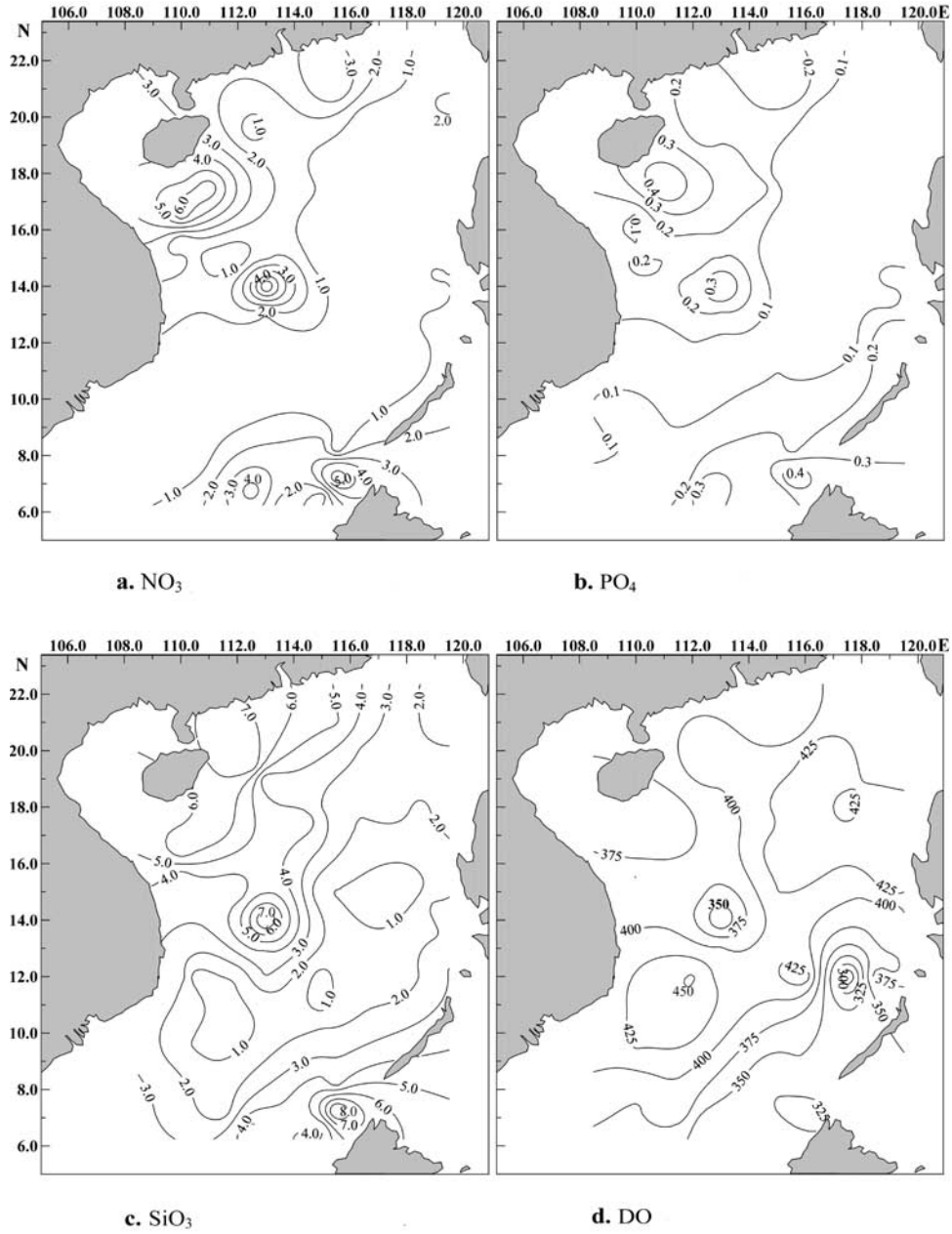

Figure 3. (a) Nitrate, (b) phosphate, (c) silicate, and (d) dissolved oxygen concentrations in the SCS at 75 m, summer 1998. Contour values are in μmol·dm^{-3}.

4.2.2. Phytoplankton Cell Abundance and Dominant Species

[24] A total of 119 species in 54 genera and 5 phylums was identified in the study area, among which 63.0% of 119 species were diatoms, 24.1% dinoflagellates, 9.3 Cyanophyta, 1.8% Chlorophyta, and 1.8% Chrysophyta. The two latter ones were observed only in the summer (Table 3). Phytoplankton abundance was 10 times higher in winter than in summer. Diatoms were the most dominant group. Furthermore, the proportion of diatoms in the phytoplankton assemblage was higher in winter (95.7%) than in summer (75.9%); that is, more non-diatoms appeared in summer than in winter (Table 3).

[25] During summer, phytoplankton abundance ranged from 0.09 $\times$ 10^3 (at Station 019) to 24.60 $\times$ 10^3 cell dm^{-3} (at Station 001), (mean = 0.84 $\times$ 10^3 cell dm^{-3}, Table 3). The highest values (>5 $\times$ 10^3 cell dm^{-3}) were in the east and northeast of Hainan Island (dominated by diatoms); high values (>1 $\times$ 10^3 cell dm^{-3}) were encountered in the southwest of Taiwan (dominated by both dinoflagellates and cyanophytes) and the northwest of Borneo (dominated by cyanophytes); intermediate values (>0.5 $\times$ 10^3 cell dm^{-3}) were encountered off the Pearl River estuary, the east off Vietnam, the basin area of the SCS (dominated by diatoms), and the northwest of Borneo (dominated by cyanophytes). In the other areas, phytoplankton abundance was <0.5 $\times$ 10^3 cell dm^{-3} (Figure 5a). The species composition in the SCS were dominated by diatoms: *Thalassiothrix frauenfeldii* Grun., *Thalassionema nitzschioides* (Grun.) V. H., *Skeletonema costatum* (Grev.) Cleve, *Pseudonitzschia*

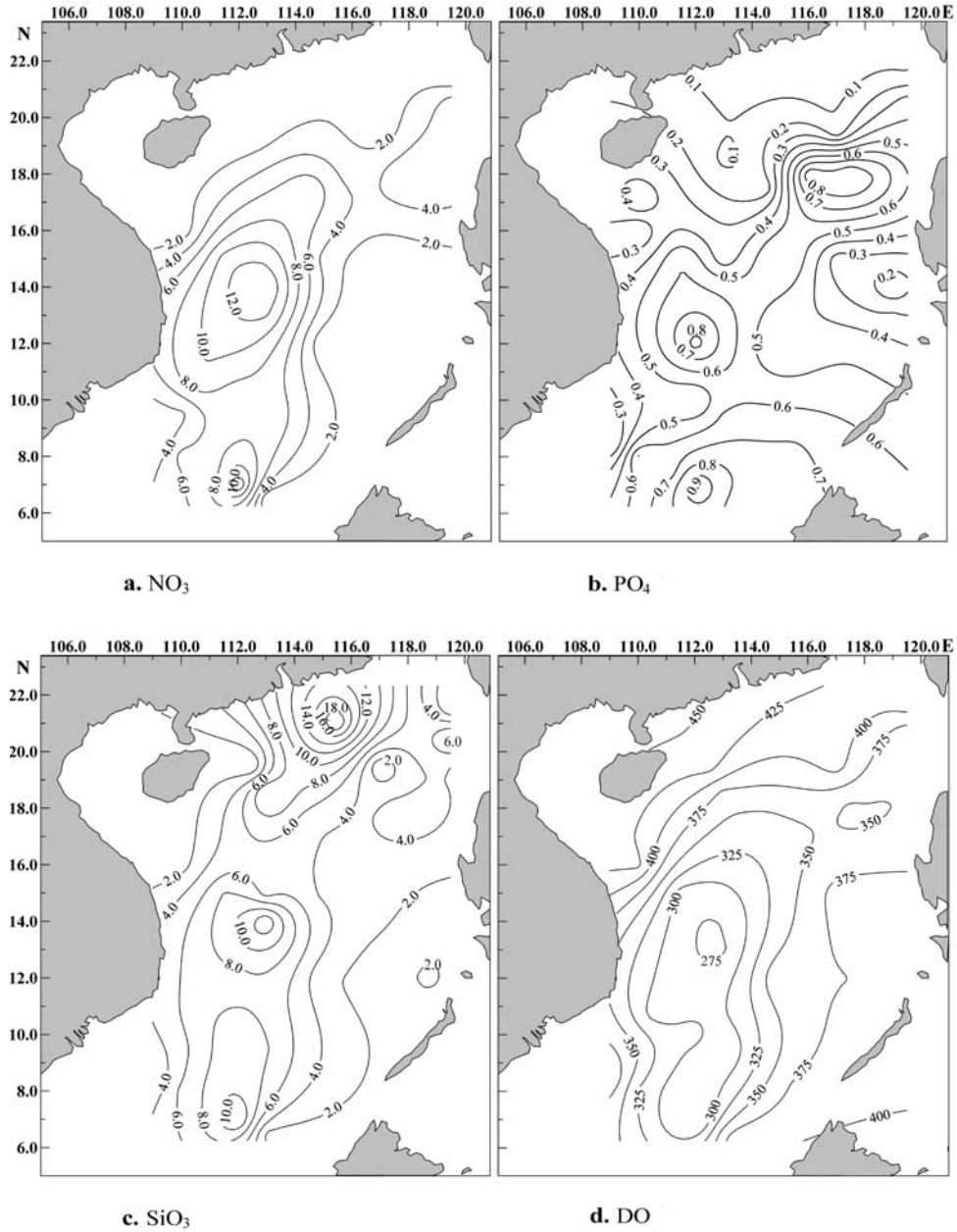

Figure 4. Similar to Figure 3, but for the winter 1998.

delicatissima (Cleve) Heiden, *Chaetoceros brevis* Schuett, *Cyclotella stylorum* Brightw., *Dactyliosolen mediterraneus* (Per.) Per., *Thalassiosira* sp., *Nitzschia* sp., etc.; dinoflagellates: *Pyrophacus horologium* Stein, *Scrippsiella trochoidea* (Stein) Balech, *Gonyaulax turbynei* Murry & Whitting, *Gonyaulax* sp., *Peridinium minutum* Kofoid, *Peridinium* sp., *Prorocentrum* sp., etc. and Cyanophyta: *Trichodesmium thiebautii* Gomont, *T. hildebrandtii* (Gom.) J. De Toni, *Oscillatoria* sp., etc.

[26] In winter, phytoplankton abundance was much higher than in summer. It ranged from 0.26×10^3 (at Station 061) to 65.62×10^3 cell dm^{-3} (at Station 041) with a mean of 8.46×10^3 cell dm^{-3} (Table 3). The high values ($>10 \times 10^3$ cell dm^{-3}) were encountered in the northern coast and shelf, the northwest of Luzon, the basin area off Vietnam, and the Sunda Shelf break (Figure 6b), and the phytoplankton were dominated by diatoms, while in the central and southeastern areas, phytoplankton abundances were low, mostly $<0.5 \times 10^3$ cell dm^{-3}, and dominated by both diatoms and dinoflagellates. The dominant species were diatom: *Thalassiothrix frauenfeldii* Grun., *T. longissima* Cleve et Grunow, *Pseudonitzschia pungenns* (Grun.) Heiden, *P. delicatissima* (Cleve) Heiden, *Thalassionema nitzschioides* (Grun.) V. H., *Thalassiosira subtilis* (Ostenf.) Gran, *Leptocylindrus danicus* Cl., *Bacteristrum commosum* Pavillard, *B. elongatum* Cleve, *B. hyalinum* Lauder, *Chaetoceros lorenzianus* Grun., *C. pseudocurvisetus* Mangin, *C. tortissimus* Gran, *C. weissflogii* Schuett, *C. denticulatus* Lauder, *Cyclotella stylorum* Brightw., *Dactyliosolen mediterraneus* (Per.) Per., *Ditylum brightwelli* (West) Grun., *Rhizosolenia stolterfothii* Per., *R. styliformis* Brightw., *Schroederella delicatula* (Perag.) Pavillard, *Skeletonema*

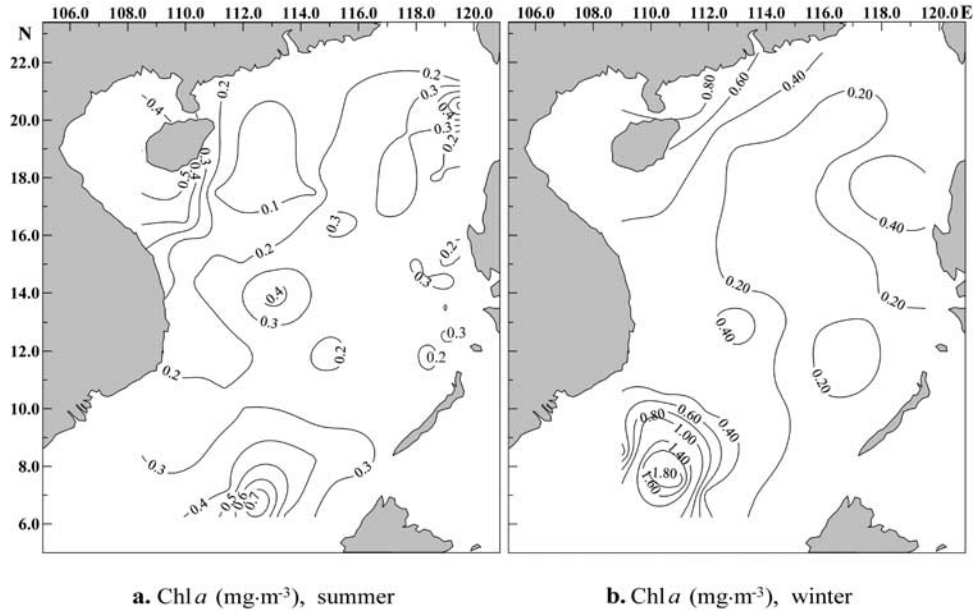

Figure 5. Concentrations (mg m^{-3}) of Chl *a* in the SCS at 75 m for (a) summer 1998 and (b) winter 1998.

costatum (Grev.) Cleve, *Eucampia cornuta* (Cleve) Grun., *Navicula* sp., etc.; dinoflagellates: *Gonyaulax minuta* Kofoid & Michener, *Prorocentrum balticum* (Lohm.) Loeb., *P. triestinum* Schiller, etc., and Cyanophyta: *T. Trichodesmium hildebrandtii* (Gom.) J. De Toni, *T. Thiebautii* Gomont, *Phormidium tenue* (Menegh.) Gom., etc.

[27] Most of the phytoplankton species found in the SCS, such as *Chaetoceros*, *Rhizosolenia*, *Pseudonitzschia*, *Thalassionema nitzschioides*, *Thalassiothrix frauenfeldii*, *Trichodesmium*, etc. (mainly diatoms up to 88 species) are wide-spread species, some others, such as *Protoperidinium*, *Gonyaulax*, *Trichodesmium*, etc. (mainly dinoflagellates up to 33 species) are warm-water species and a few, for example, *Prorocentrum* and two other species of dinoflagellates, are temperate species.

4.3. Primary Production (PP)

[28] During summer, PP ranged from 94.5 (at Station 101) to 1305.8 mg C m^{-2} d^{-1} (at Station 044) (mean = 389.8 mg C m^{-2} d^{-1}, Table 1). High values (>400 mg C m^{-2} d^{-1}) were mainly in the areas north of the Sunda Shelf, east of Vietnam, and southeast of Hainan Island, while low values (<200 mg C m^{-2} d^{-1}) were encountered in the northern continental shelf and west of Luzon (Table 4). During winter, PP was higher than in summer and ranged from 145.8 (at Station 103) to 1605.4 mg C m^{-2} d^{-1} (at Station 041) (mean = 546.0 mg C m^{-2} d^{-1}, Table 1). High values (>500 mg C m^{-2} d^{-1}) were observed northwest of Luzon, in the basin area of the SCS and the Sunda Shelf (Table 4).

4.4. Size-Fractionated Chl *a* and PP

[29] In summer, the average contributions of net-, nano-, and pico-plankton to the biomass of phytoplankton communities were 6, 17, and 77%, respectively (Table 5), and the contribution order was pico- $\gg$ nano- > net- fractions. In winter, the average contributions of net-, nano-, and pico-plankton to the biomass of phytoplankton communities were 35, 12, and 53%, respectively, and the order was pico > net > nano (Table 5). The average contributions of net-, nano-, and pico-plankton to PP were 24, 33, and 42%, respectively, in summer, and 21, 22, and 57%, respectively, in winter (Table 5).

5. Discussion

[30] The primary objectives of this study were to understand how phytoplankton dynamics associate with the physical, chemical, and biological coupling oceanography processes in the SCS and how they respond to monsoons.

Table 3. Number of Species (SN), Frequency of Occurrence (OF), and Average Abundance (AA) of Various Phylums of Phytoplankton in the SCS in 1998

	Summer (n = 61)					Winter (n = 49)				
	SN			AA		SN			AA	
Phylum	Number	Percent	OF, %	$\times 10^3$ cell dm^{-3} (±SD)	Percent	Number	Percent	OF, %	$\times 10^3$ cell dm^{-3} (±SD)	Percent
Bacillariophyta	49	55.7	62.7	0.63 ± 2.18	75.9	61	71.8	93.9	8.10 ± 12.64	95.7
Pyrrophyta	30	34.1	50.8	0.09 ± 0.16	10.8	22	25.8	36.7	0.16 ± 0.25	1.9
Cyanophyta	7	8.0	32.8	0.11 ± 0.25	13.3	2	2.4	6.1	0.20 ± 1.19	2.4
Chlorophyta	1	1.1	1.6	<0.01		0	0	0	0	0
Chrysophyta	1	1.1	1.6	<0.01		0	0	0	0	0
Sum	88	100		0.84 ± 0.86	100	85	100		8.46 ± 4.69	100

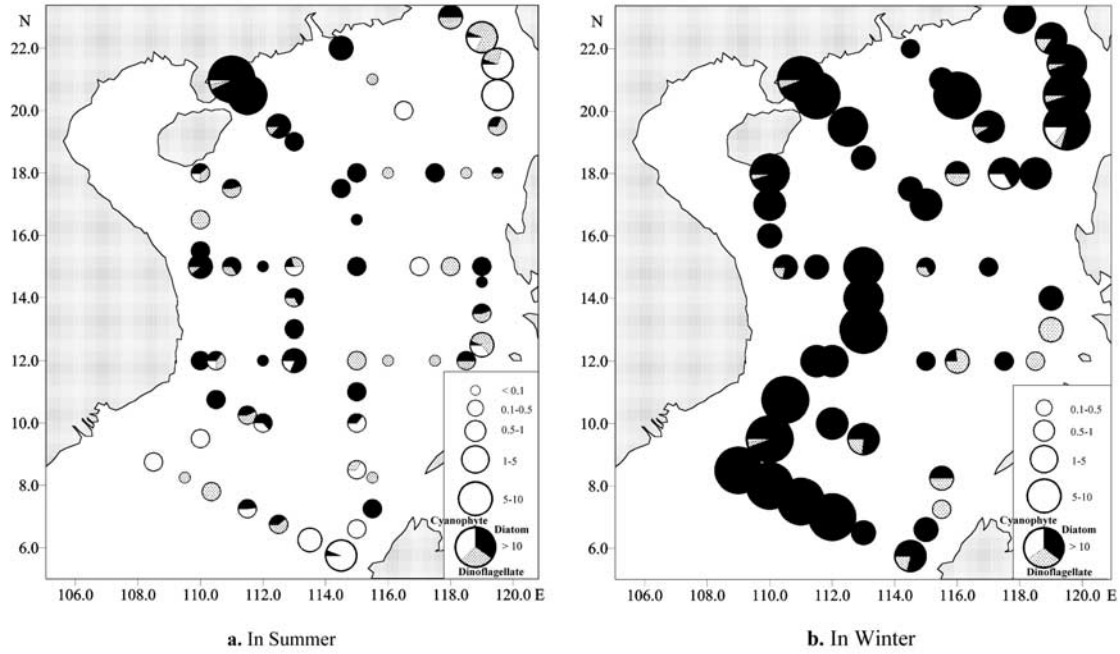

Figure 6. Phytoplankton abundance (Phyt. Abund. $\times$ 10^3 cell dm^{-3}) in the SCS for (a) summer 1998 and (b) winter 1998.

Despite the fact that the phytoplankton data used in this study were obtained from only two large spatial scale survey cruises in the SCS, several important results arise.

5.1. Summer Upwelling Along the Southern Coast of China

[31] In summer, under the southwesterly monsoon forcing the whole SCS was generally controlled by a basin-wide anti-cyclonic gyre. In the western, northwestern, and northern parts of the SCS, the current flowed along the Vietnam coast, the south and east coasts of Hainan Island, and the China mainland coast. Wind-induced ''Ekman transport'' moved the surface water away from the coast, and cold and saline subsurface water upwelled [*Xue et al.*, 2001a], resulting in low temperature (<22°C, Figure 2a), high salinity (>34.6, Figure 2b), relatively high concentrations of nutrients (e.g., in general, NO_3 > 2.0 μmol dm^{-3}, PO_4 > 0.2 μmol dm^{-3}, and SiO_3 > 5.0 μmol dm^{-3}, Figures 3a–3c) and low DO (<400 μmol dm^{-3}, Figure 3d). Chl *a* distribution in the regions showed relatively high values (>0.2 mg m^{-3}) in the surface water and relatively low values (<0.2 mg m^{-3}) at the depth of 75 m (Figures 5a and 7d), which was below the euphotic zone where the light became a limiting factor for phytoplankton growth in the northern coast and shelf regions. The influence of coastal upwelling induced by the Ekman transport [*Xue et al.*, 2001a] and the Pearl River discharges were clearer from the vertical distributions of the various parameters on the transect: Station 103 to Station 084 (Figure 7). The isopleths of temperature, salinity, and NO_3 uplifted along the coast of the northern SCS, resulting in a decrease in temperature, and an increase in salinity and NO_3 near the shelf-break. In the upper layer, the hydrographic, chemical, and biological properties were also influenced by fresh water discharge from rivers, particularly the Pearl River, shown as a low-salinity (<34) layer in the upper 20 m. In general, the concentration of Chl *a* was high in the upwelling zone between Stations S103 and S101 and from the surface down to about 90 m. The Chl *a* maximum appeared right underneath the low-salinity lens, due to high vertical water stability, resulting from a strong and shallow halocline and thermocline.

[32] The Ekman transport associated with the southerly and southwesterly monsoon induced another upwelling region: a mesoscale cyclonic cold eddy located to the southeast of Hainan Island [*Chai et al.*, 2001b]. This CE was characterized by low temperature (<21°C, Figure 2a), high salinity (>34.6, Figure 2b), high nutrients (e.g., NO_3 > 3.0 μmol dm^{-3}, PO_4 > 0.3 μmol dm^{-3}, and SiO_3 > 6.0 μmol dm^{-3}, Figures 3a–3c), low DO (<375 μmol dm^{-3}, Figure 3d) and relatively high Chl *a* concentrations (>0.3 mg m^{-3}, Figure 5a). The strongest upwelling appeared at the location between S009 and S012, where lower temperature and higher concentrations of nutrients were encountered at a depth of 75 m (Figure 8). Concentrations of NO_3, PO_4 and Chl *a* were 2 times higher in the upwelling zone than offshore. The low-salinity lens at the surface could be the remnant of the westward branch of the Pearl River plume in the summer. Again, the Chl *a* maximum occurred immediately underneath the low-salinity lens.

5.2. Summer Downwelling Along the Eastern Wall of the SCS Basin

[33] The highest SST (>30.8°C), however, appeared in the eastern and southeastern SCS, especially northwest of Palawan Island and west of Luzon (>31.0°C at the surface, and T > 26°C at the depth of 75 m, Figure 2a), which was probably caused by the inflow from the Sulu Sea. Correspondingly, nutrient concentrations were low (e.g., NO_3 < 1.0 μmol dm^{-3}, PO_4 < 0.2 μmol dm^{-3}, and

Table 4. Primary Production (PP) and its Relationship With the Mesoscale Eddies in the SCS in 1998[a]

Station	Location	Water Mass Features	PP, mg Cm^{-2} d^{-1}
		Summer	
004	WP	Relatively high temp. (>22°C), relatively low sal. (<34.4), low nutrients (NO_3 < 1 μmol dm^{-3}, PO_4 < 0.2 μmol dm^{-3}), high DO (>400 μmol dm^{-3}), and low Chl *a* (<0.1 mg m^{-3})	105.5
012	CE	Low temp. (<21°C), high sal. (>34.6), high nutr. (NO_3 > 6 μmol dm^{-3}), low DO (<375 μmol dm^{-3}), and relatively high Chl *a* (>0.2 mg m^{-3})	450.9
021	CE	Low temp. (<21°C), high sal. (>34.6), high nutrients (NO_3 > 6 μmol dm^{-3}), low DO (<350 μmol dm^{-3}), and high Chl *a* (>0.4 mg m^{-3})	753.6
024	WP	High temp. (>24°C), relatively low sal. (<34.3), low nutrients (NO_3 < 1 μmol dm^{-3}, PO_4 < μmol dm^{-3}), high DO (>400 μmol dm^{-3}), and low Chl *a* (<0.2 mg m^{-3})	232.9
034			231.0
044	UW (Sunda shelf break)	Low temp. (<22°C), high sal. (>34.4), high nutr. (NO_3 > 4 μmol dm^{-3}), low DO (<350 μmol dm^{-3}), and high Chl *a* (>0.4 mg m^{-3})	1305.8
056			423.1
061			233.9
067	WP	High temp. (>26°C), relatively low sal. (<34.5), low nutr. (NO_3 < 1 μmol dm^{-3}, PO_4 < 0.1, high DO (>400 μmol dm^{-3}), and relatively low Chl *a* (<0.2 mg m^{-3})	181.1
079			227.9
091			436.8
101			94.5
Mean (SD)			**389.8 (342.5)**
		Winter	
008			508.9
016			372.9
021	CE	Low temp. (<19°C), high sal. (>34.6), high nutr. (NO_3 > 12 μmol dm^{-3}), low DO (<275 μmol dm^{-3}), and relatively high Chl *a* (>0.4 mg m^{-3})	789.0
041	UW	Low temp. (<21°C), high sal. (>34.4), high nutr. (NO_3 > 6 μmol dm^{-3}), low DO (<300 μmol dm^{-3}), and relatively high Chl *a* (>1.8 mg m^{-3})	1605.4
048			403.4
061			438.9
068			438.3
078	WP	Relatively high temp. (>21°C), relatively low sal. (<34.6), low nutr. (NO_3 < 1 μmol dm^{-3}, PO_4 < 0.1, high DO (>425 μmol dm^{-3}), and relatively low Chl *a* (<0.2 mg m^{-3})	244.4
084	CE	Low temp. (<21°C), high sal. (>34.6), high nutr. (NO_3 > 4 μmol dm^{-3}), low DO (<350 μmol dm^{-3}), and relatively high Chl *a* (>0.5 mg m^{-3})	513.4
103			145.8
Mean (SD)			**546.0 (409.4)**

[a]CE: Cold eddy; WP: Warm pool; UW: Upwelling.

SiO_3 < 2.0 μmol dm^{-3}, Figures 3a–3c), DO was high (>425 μmol dm^{-3}, Figure 3d), Chl *a* concentration were low (0.2 mg m^{-3}, Figure 5a and Table 2a) and phytoplankton abundance was low (<0.5 × 10^3 cell dm^{-3}, Figure 6a), probably due to the wind-induced downwelling along the eastern wall of the basin [*Shaw and Chao*, 1994; *Udarbe-Walker and Villanoy*, 2001; *Liu et al.*, 2002].

5.3. Mesoscale Warm Pools (WP) and Cold Eddies (CE) in the Summer

[34] The summer distribution of temperature (Figure 2a) shows a distinct pattern of alternating warm and cold patches. They were actually associated with mesoscale cyclonic and anti-cyclonic eddies, formed in response to the combined effects of monsoon, topography, and shape of the coastal line and the inertial effects [*Zeng et al.*, 1989; *Xu et al.*, 2001]. These mesoscale cyclonic and anti-cyclonic eddies were confirmed by ADCP (Acoustic Doppler Current Profiler) surveys [*Xu et al.*, 2001] and satellite-tracked surface drifting buoys and satellite-derived sea surface height [*Morimoto et al.*, 2000]. The cyclonic gyre induced local upwelling and resulted in a cold eddy, while the anti-cyclonic gyre induced local downwelling and resulted in a warm pool [*Su et al.*, 1999].

[35] Several pronounced warm pools existed in the areas southeast of Vietnam between Stations S028 and S023, and east of Hainan Island centered at Station 04 (Table 2a). Vertical distributions of the temperature, salinity, NO_3, and Chl *a* (not shown) indicated clearly a downwelling center between S028 and S024, a relatively strong halocline between 75 m and 125 m, and the depletion of nitrate in the upper 75 m. Similarly, nitrate was depleted and Chl *a* concentration was low in the upper 75 m at S004, the center of the downwelling associated with the WP east of Hainan.

Table 5. Size-Fractionated Chlorophyll *a* (Chl *a*) and Primary Production (PP) at the Surface and 75 m in the SCS in 1998

		Summer		Winter	
Parameter	Size-Fraction	Surface (n = 61)	75 m (n = 56)	Surface (n = 49)	75 m (n = 46)
Chl *a*, μg dm^{-3}	net	0.02 ± 0.03 (16%)	0.02 ± 0.02 (6%)	0.10 ± 0.28 (36%)	0.13 ± 0.31 (35%)
	nano	0.02 ± 0.03 (22%)	0.04 ± 0.03 (17%)	0.04 ± 0.05 (14%)	0.04 ± 0.07 (12%)
	pico	0.07 ± 0.04 (63%)	0.20 ± 0.12 (77%)	0.15 ± 0.09 (51%)	0.19 ± 0.09 (53%)
	sum	0.11 ± 0.07 (100%)	0.26 ± 0.16 (100%)	0.29 ± 0.34 (100%)	0.36 ± 0.41 (100%)
PP,[a]	net	94.0 ± 59.0 (n = 12) (24%)		112.2 ± 227.9 (n = 10) (21%)	
mgC m^{-2} d^{-1}	nano	130.1 ± 281.1 (n = 12) (33%)		120.1 ± 131.3 (n = 10) (22%)	
	pico	165.6 ± 153.4 (n = 12) (42%)		313.7 ± 144.8 (n = 10) (57%)	
	sum	389.8 ± 342.5 (n = 12) (100%)		546.0 ± 409.4 (n = 10) (100%)	

[a]Daily integrated primary production within euphotic zone.

[36] On the contrary, a strong cold eddy existed off the east coast of Vietnam in the central SCS (Stations 021, 022, Figures 2a, 2b, 9a, and 9b) lay between the previously described warm pools. This cold eddy, and hence the upwelling, must be induced by the separation of the western boundary current from the Vietnam coast [*Liu et al.*, 2002]. A similar upwelling in the North Atlantic Ocean was reported by *Csanady and Hamilton* [1988] at the location where the Gulf Stream separates from the coast near Cape Hatteras. Upwelling in the cold eddy supplies nutrients to the upper water column, which in turn gives rise to the increase in concentration of Chl *a* and primary production. Unlike the coastal upwelling due to winds, upwelling associated with cold eddies might start from greater depths.

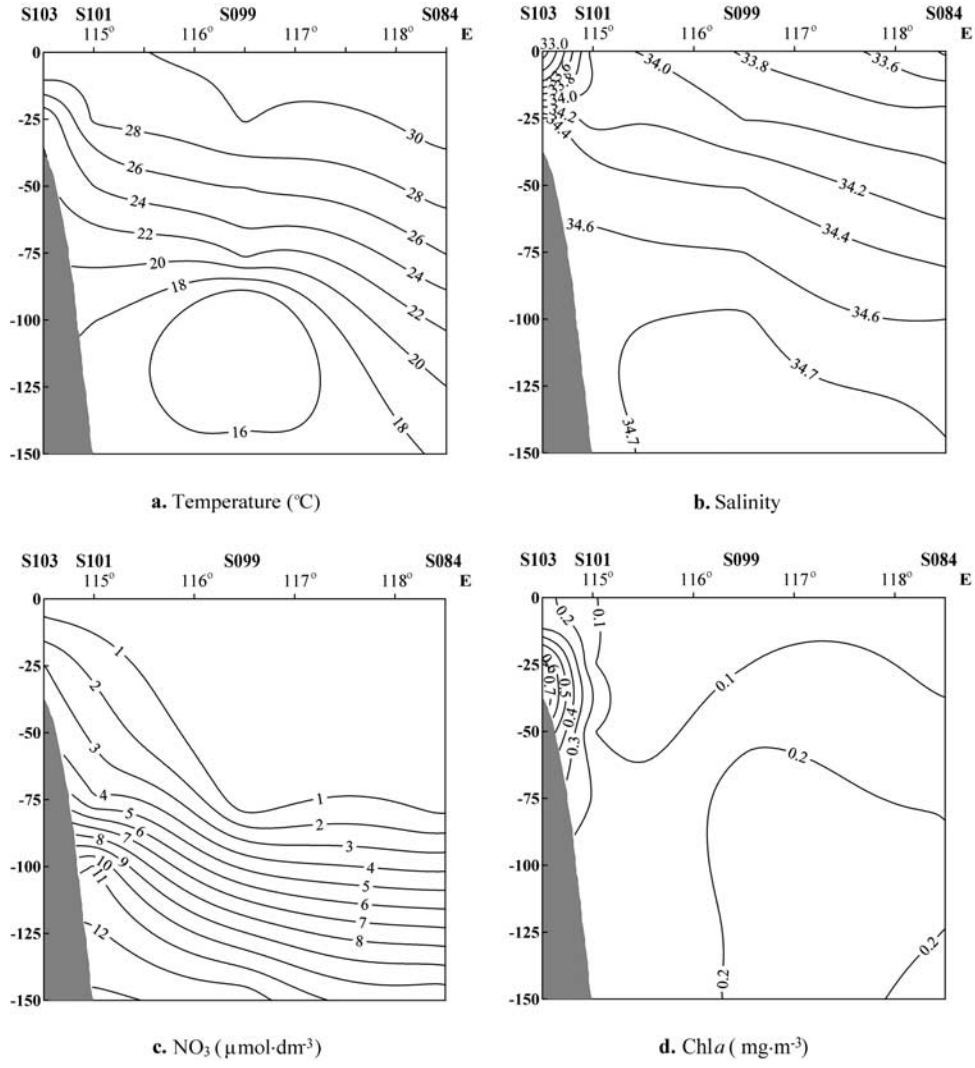

Figure 7. Vertical distributions of (a) temperature, (b) salinity, (c) nitrate, and (d) Chl *a* concentrations on the transect between S103- and S084 during summer 1998 showing northern coastal and shelf upwelling resulted from Ekman transport induced by the southwest monsoon, and the influence of the Pearl River discharge.

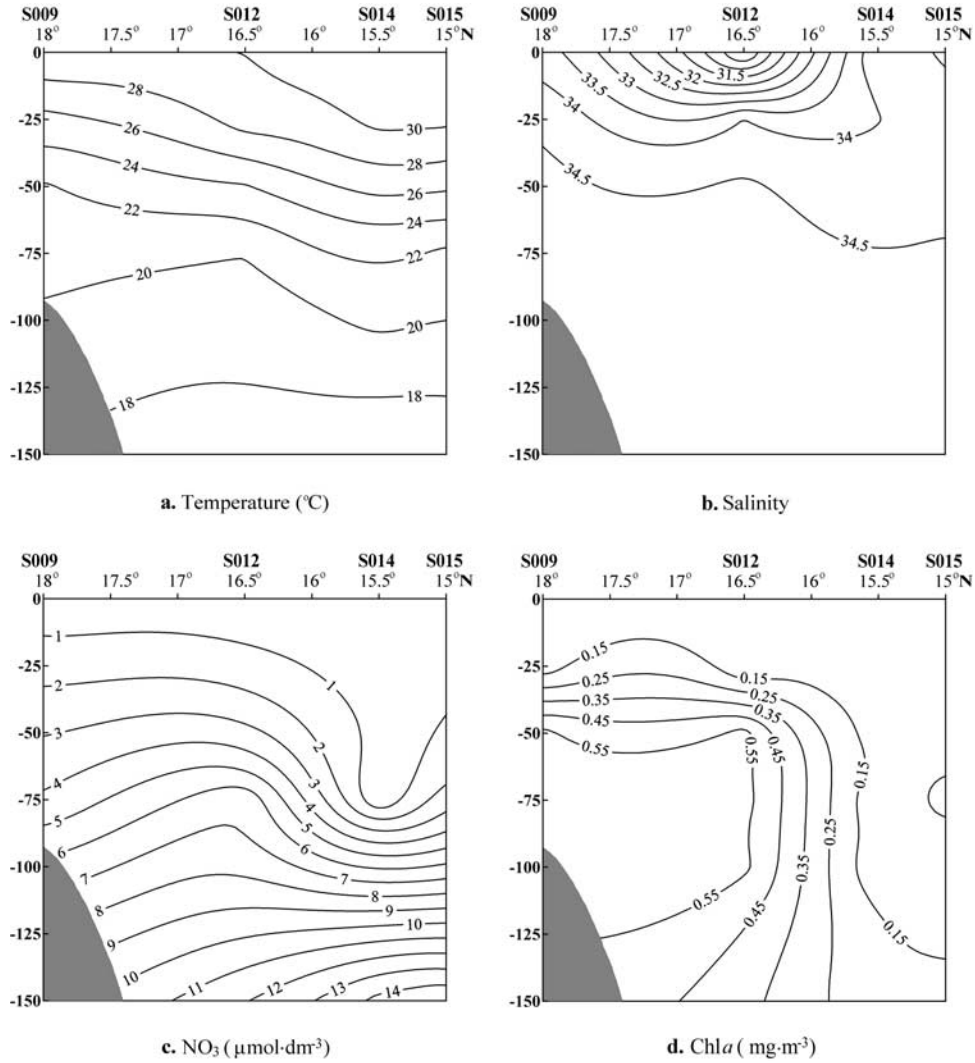

Figure 8. Similar to Figure 7, but for the transect between S009 and S015, showing the strong upwelling center (southeast of Hainan Island), and the strong stratification of the water column.

In this cold eddy, upwelling was centered between S021 and S022. The water came from below 150 m, and the signature could be traced at the surface. The maximum concentration of Chl *a* (>0.45 mg m^{-3}) occurred at 75 m, where the water mass was characterized by low temperature (<21°C), high salinity (>34.6), relatively high nutrient concentration (e.g., NO_3 > 4.0 μmol dm^{-3}, PO_4 > 0.2 μmol dm^{-3}, and SiO_3 > 4.0 μmol dm^{-3}, Figures 3a, 3b, 3c, and 9) and low DO (<400 μmol dm^{-3}, Figure 3d). The primary production was 753.6 mg C m^{-2} d^{-1} at S021 (Table 4). This finding was similar in magnitude to the results of *Vaillancourt et al.* [2003] obtained in the eddy Haulani near Hawaii.

[37] North of the Sunda Shelf in the southern SCS, high Chl *a* concentrations (>0.5 mg m^{-3}, Figure 5a) resulted from relatively high nutrient concentrations (e.g., NO_3 > 2.0 μmol dm^{-3}, PO_4 > 0.2 μmol dm^{-3}, and SiO_3 > 3.0 μmol dm^{-3}, Figures 3a–3c), induced by the so-called "Wanan Cyclonic Gyre" [*Fang et al.*, 1998]. The maximum uplift of isotherms appeared near S042 (Figure 10a). However, the uplift of nutrient isopleths, and consequently, the maximum concentration of Chl *a,* occurred between S044 and S048 (Figures 10c and 10d). This eddy was shallower, and extended to only about 125 m. The highest concentration of Chl *a* (>0.5 mg m^{-3}) occurred at 75 m and this upwelling was associated with the highest level of primary production (1305 mg C m^{-2} d^{-1} at Station 044) among all the measurements during the summer (Table 4). Finally, the Mekong River plume was observed near S042 in the upper 20 m (Figure 10b).

5.4. Winter Cyclonic Gyre in the Central Basin

[38] When the winter monsoon peaks in December, there formed a basin-wide cyclonic gyre. In the northeast the gyre connected with the cold eddy northwest of Luzon, while to the south it was connected with another cold eddy north of the Sunda Shelf. Together they formed a pronounced long cold trough with a northeast-southwest directional axis (Figures 2c and 2d). The cyclonic gyre situated between 9°N and 18°N and between 109°E and 116°E, detectable from both the TOPEX/Poseidon (T/P) altimetry data [*Wang et al.*, 1999] and the XBT data [*Metzger and Hurlburt*, 1996], induced a strong upwelling in the central basin of the SCS. The center of the upwelling was located at 111°E–114°E, between S016 and S076 (Figure 11). From the

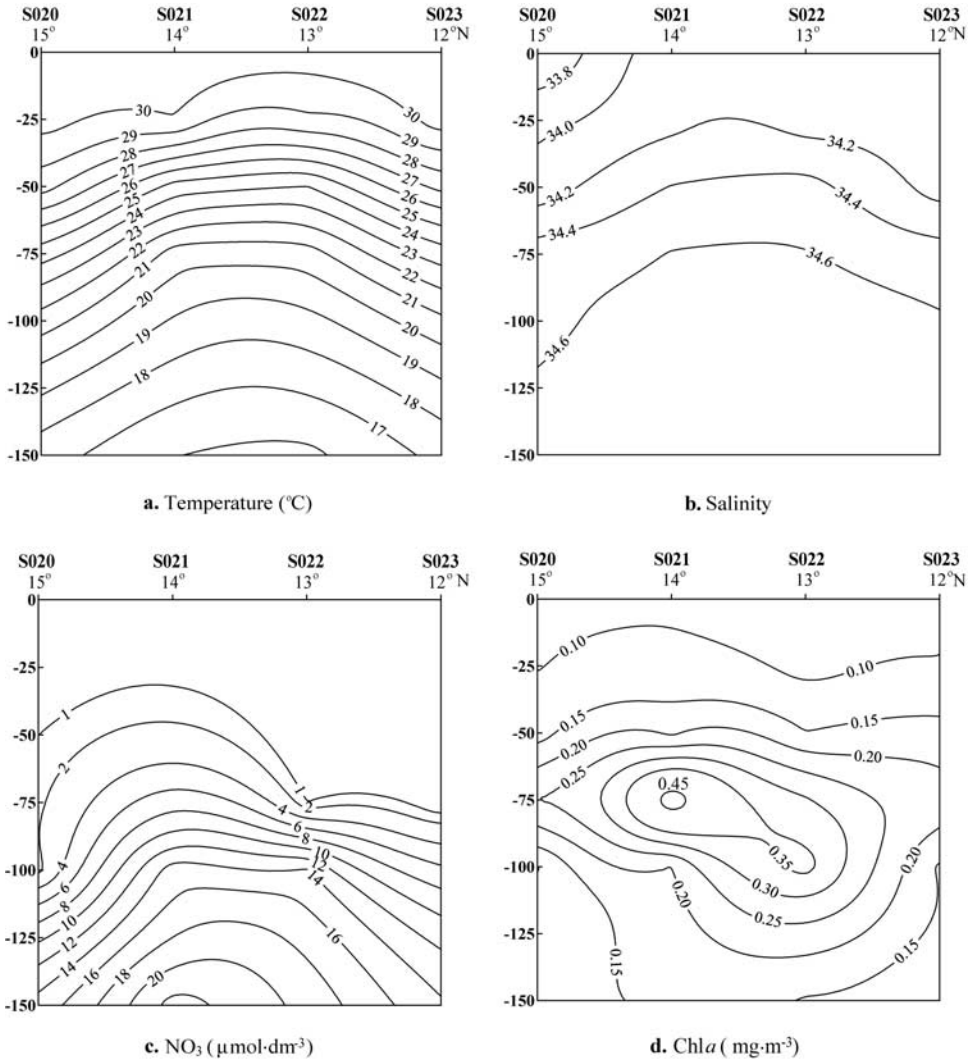

Figure 9. Similar to Figure 8, but for the transect between S020 and S023, showing the upwelled water associated with the cold eddy off Vietnam, and the corresponding subsurface chlorophyll maximum (SCM).

transect, it is clear that the water moved up from below 150 m and the upwelled water was characterized by low temperature, high salinity, high nutrients, and a low DO concentration (Table 2b). At 75 m of the upwelling area where the maximum Chl *a* concentration appeared, the temperature was 2°C colder and NO_3 concentration was 2.0 μmol dm^{-3} higher than that of the surrounding waters.

5.5. Mesoscale Cold Eddies in the Winter

[39] The cold eddy or local upwelling northwest of Luzon might be induced by a subsurface convergence of a northward jet off the west coast of Luzon [*Shaw et al.*, 1996] and by Ekman suction driven by local wind stress during winter monsoon [*Chao et al.*, 1996; *Chai et al.*, 2001a]. Characterized by the cold (<21°C, Figure 2c) and saline (>34.6, Figure 2d) water with high nutrient concentrations (NO_3 > 4.0 μmol dm^{-3}, PO_4 > 0.8 μmol dm^{-3}, and SiO_3 > 4.0 μmol dm^{-3}, Figures 4a–4c), low DO (<350 μmol dm^{-3}, Figure 4d), and relatively high Chl *a* concentrations (>0.4 mg m^{-3}, Figure 5b), this upwelling was also clearly seen from the vertical distributions of the properties on the transect from Station 101 to 084 (Figure 12). At S084, the central area of the upwelling, the isopleths of temperature, salinity, and nitrate uplifted, resulting in a shallower mixed layer, and higher nutrient concentrations, and therefore higher Chl *a* concentration (>0.55 mg m^{-3}) at a shallower depth of 60 m. The upwelling water with high nutrients spread southwestward along the cold trough and become an important nutrient source in the interior of the SCS [*Shaw et al.*, 1996], supplying it to the euphotic zone for phytoplankton growth.

[40] At the southern end of the cold trough, an area of high Chl *a* (>1.0 mg m^{-3}, Figure 5b) and high phytoplankton abundance (>20 × 10^3 cell dm^{-3}, Figure 6b) were observed north of the Sunda Shelf. This region is relatively low in latitude with a diminishing Coriolis force. When the southward current impinged upon the Sunda Shelf, it was uplifted by the shoaling topography of the seafloor, reinforcing the upwelling induced by the cyclonic gyre. *Chu et al.* [1997] reported a strong negative SST anomaly of 1.8°–2.4°C in winter months to the southeast of Vietnam in a

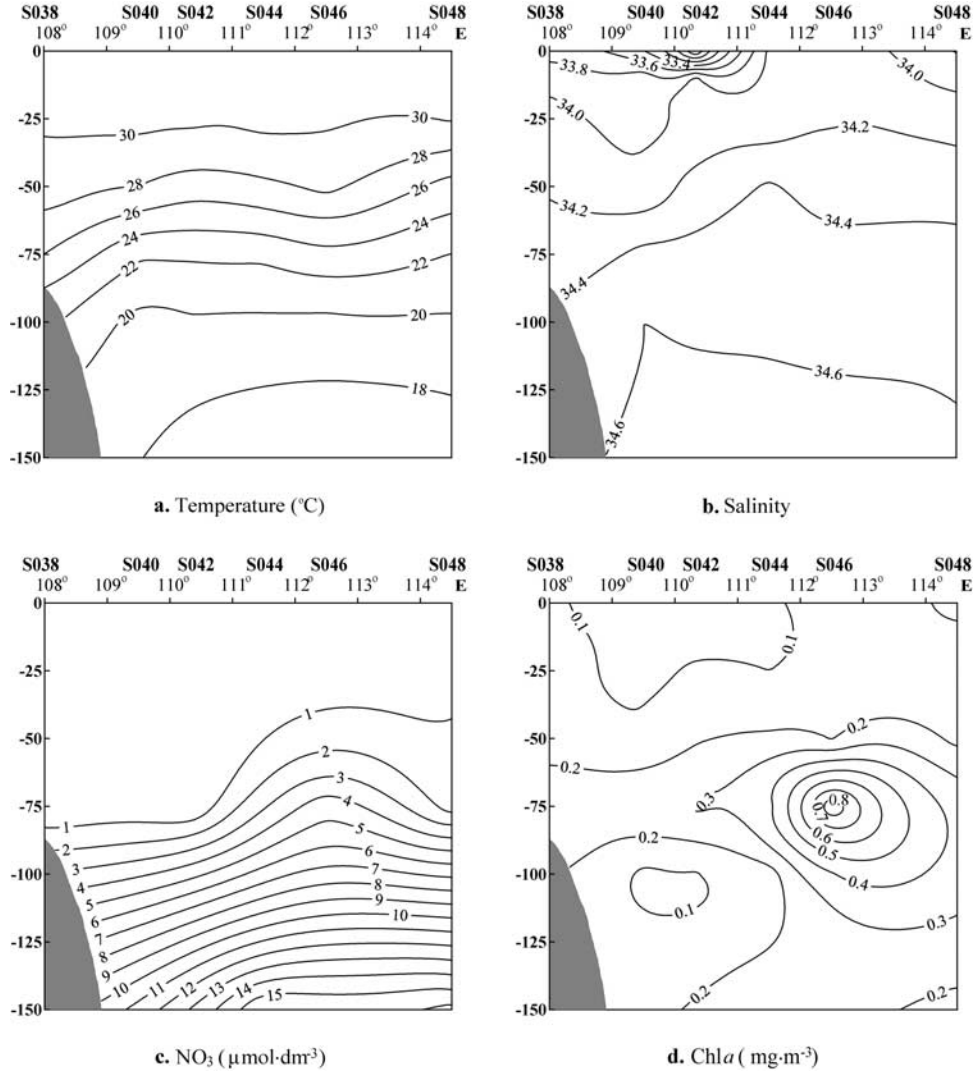

Figure 10. Similar to Figure 8, but for the transect between S038 and S048, showing the upwelling north of the Sunda Shelf (from S044 to S048), and the corresponding SCM at the bottom of the euphotic zone, as well as the Meikong River plume around S042.

close proximity of this upwelling area. The center of the upwelling was located near S041, where the cold (<24°C), saline (>34), and nutrient-rich (NO_3 > 7 μmol dm^{-3}) water upwelled (Figures 13a–13c). The upwelled water met with the warm and fresher upper layer water at the depth of about 50 m, resulted in a strong thermocline and halocline within the euphotic zone. Phytoplankton bloomed and a strong subsurface Chl *a* maximum (SCM) with concentration >1.6 mg m^{-3} appeared (Figure 13d). Interestingly, having the maximum concentration of NO_3 at 75 m indicated a possible lateral source of nutrients being delivered to this region, which is probably the reason that the primary production reached the highest level (1605.4 mg C m^{-2} d^{-1}, at Station 041) during both winter and summer seasons (Table 3).

5.6. Intrusion Through the Luzon and the Mindora Straits

[41] Driven by the northeasterly monsoon, a warm and saline water mass (T > 25°C and S > 34.7, Figures 2c and 2d) was encountered in the area southwest of Taiwan, reflecting the intrusion of Kuroshio from the west Pacific to the SCS through Luzon Strait [*Fang et al.*, 1998; *Xue et al.*, 2004]. The Kuroshio water had relatively low nutrient concentrations (e.g., NO_3 < 2.0 μmol dm^{-3}, PO_4 < 0.2 μmol dm^{-3}, and SiO_3 < 3.0 μmol dm^{-3}, Figures 4a–4c) and low Chl *a* (<0.3 mg m^{-3}, Figure 5b). It flowed westward along the northern shelf margin of the SCS [*Shaw*, 1991].

[42] Along the eastern shore of the SCS, a jet consisting of warm (>25°C, Figure 2c) and less saline (<34.4, Figure 2d) water shot northwestward into the central basin of the SCS. This water came from the Sulu Sea. It intruded into the eastern and southeastern SCS through the Mindoro Strait, forming a low-nutrient (NO_3 < 2.0 μmol dm^{-3}, PO_4 < 0.4 μmol dm^{-3}, and SiO_3 < 3.0 μmol dm^{-3}) and low Chl (<0.2 mg m^{-3}) area (Figures 4a, 4b, 4c, and 5b).

5.7. Physical-Chemical-Biological Coupling in the SCS

[43] When the regression analysis was made between Chl *a* and the related physical and chemical parameters for

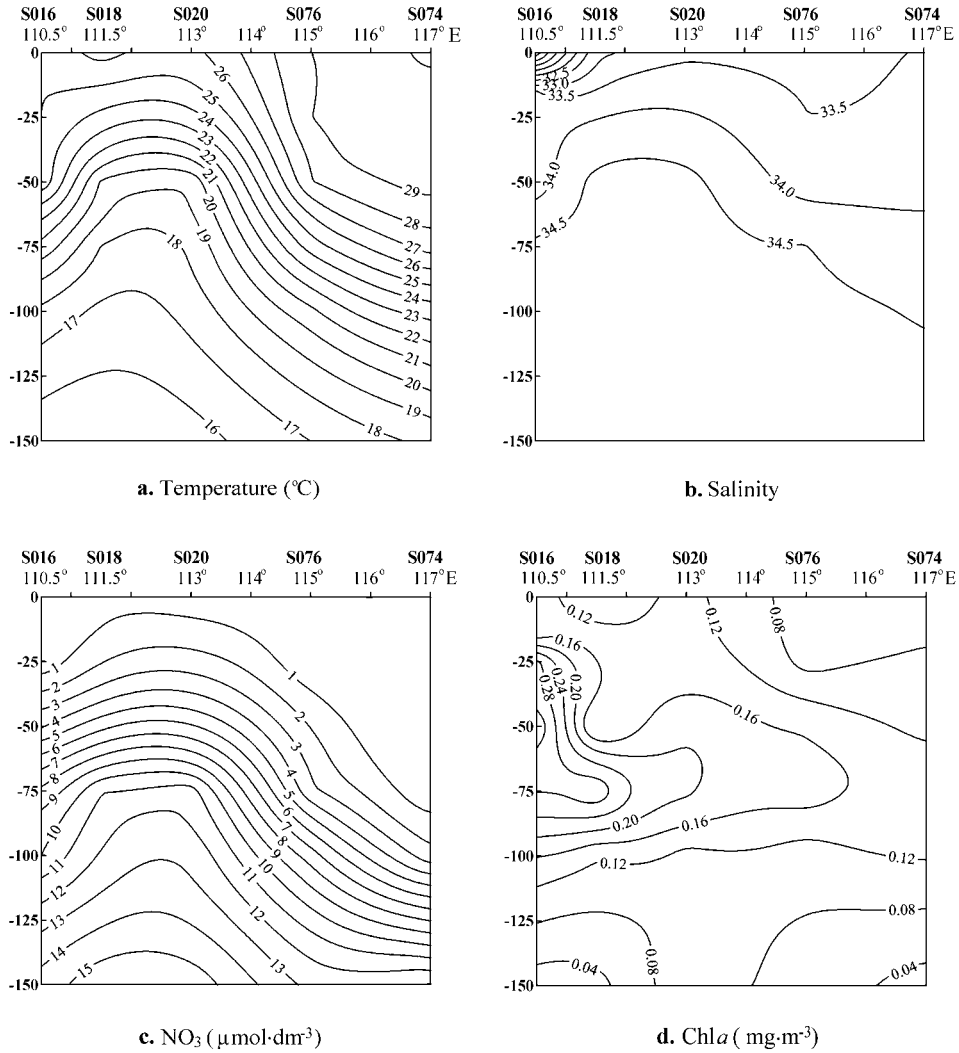

Figure 11. Vertical distributions of (a) temperature, (b) salinity, (c) nitrate, and (d) Chl *a* concentrations on the transect between S016 and S074 during the winter 1998, showing the strong upwelling east of the central Vietnam associated with the basin-wide cyclonic gyre and the corresponding SCM at the bottom of the euphotic zone.

both cold eddies and warm pools and for both seasons, strong correlations were obtained. Correlations were highly significant, particularly for summer; that is, there were strong positive correlations between Chl *a* concentration and salinity, and between Chl *a* and nutrients (NO_3, PO_4, and SiO_3), while there were negative correlations between Chl *a* and temperature, and between Chl *a* and DO (Table 6).

[44] Although the few primary production (PP) measurements obtained (Table 4) during the two cruises make it difficult to delineate the spatial and seasonal variations in PP, the data, to some extent, reflect the seasonal patterns of the coupled physical-biological processes in the SCS. In summer, high PP (>450 mg C m^{-2} d^{-1}, Table 4) occurred in the upwelling areas; low PP values (<250 mg C m^{-2} d^{-1}) appeared in the northern shelf and in the warm pools. In winter, high PP (>500 mg C m^{-2} d^{-1}) occurred in the three cold eddies; low PP values occurred at the tip of warm jet off the west coast of Luzon and near the Pearl River mouth as a result of a shallower euphotic zone (<50 m). Primary production and its relationship with the mesoscale features are summarized in Table 3.

[45] Elucidating the physical-chemical-biological characteristics associated with cold eddies is significant not only for contemporary oceanography, but also for potential development and management of living resources. Phytoplankton and zooplankton are important food for the early stage of fish, and must be abundant in cyclonic eddies, resulting from the enrichment of food, as observed by *Nishimoto and Washburn* [2002] in the Santa Barbara Channel. They found a high abundance of fish in the center of a cyclonic eddy in the western Channel corresponding to the lowest dynamic height in the study area, indicating a strong link between mesoscale flows and spatial abundance patterns of juvenile and late-stage larval fishes. Time series of relative vorticity indicated that the cyclonic eddy observed during the 1998 survey was stable, persistent feature

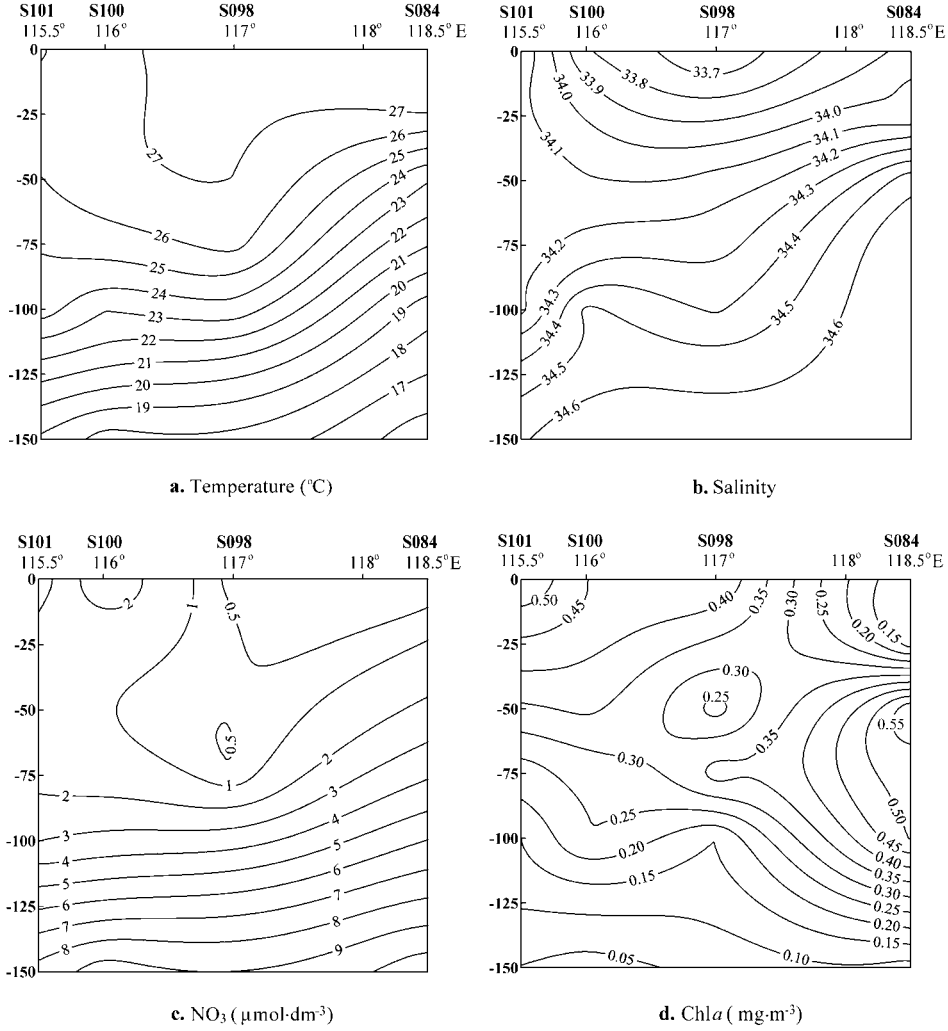

Figure 12. Similar to Figure 11, but for the transect between S101 and S084, showing the upwelling northwest of Luzon, and the corresponding strong halocline and the SCM at S084.

developing about 6 weeks before the trawling surveys. In the SCS, the persistence of the cyclonic eddy features should be closely related to seasonal monsoon forcing.

[46] Size-fractionated determination of Chl *a* and PP gave significant results. The contribution of photosynthetic picoplankton (<2 μm, in size) to the biomass of phytoplankton communities was the highest (>50%) in both summer and winter and in different layers of the water column in the SCS (Table 5). The contribution of picoplankton to PP was also the highest in both summer and winter (Table 5). The vertical distribution of Chl *a* for net- and nano-plankton was relatively uniform, while for picoplankton, its Chl *a* concentration was much higher at 75 m than at the surface (Table 5) in both seasons, and it was the primary contributor to the subsurface Chl *a* maximum (SCM). This is consistent with the previous observation in the SCS reported by *Takahashi and Hori* [1984] that more than 70% of Chl *a* in the SCM was derived from picoplankton <3 μm. Furthermore, it was also observed by using flow cytometry that the SCM was dominated by picoeukaryotes. For the horizontal distribution, the importance of *Prochlorococcus* increased seaward, while picocyanobacteria *Synechococcus* became more important nearshore and picoeukaryotes abundance was relatively low, but the Chl *a* content for the latter was much higher than the two formers, and less spatially variable [*Ning et al.*, 2003].

5.8. Nutrient Depletion and Specie Succession

[47] Nutrient depletion was also observed at the surface during summer, particularly for phosphorus in a large area extending from the southwest to the east and northeast, even at 75 m (Figure 3b). At some locations, its concentration was so low that it fell below the detection limit (0.03 μmol dm^{-3} [*Strickland and Parsons*, 1972]). For the whole studied area, the average N/P molar ratio = 42, which coincided with *Yin* [2002], who observed a ratio of 64 in the southern water of Hong Kong during summer, which played an important role for controlling biomass and production of phytoplankton. Nitrate concentrations <1 μmol dm^{-3} were also encountered in the upper layer of the water column for the same area (Figure 3a). This type of vertical distribution was probably a response to the seasonal water stratification.

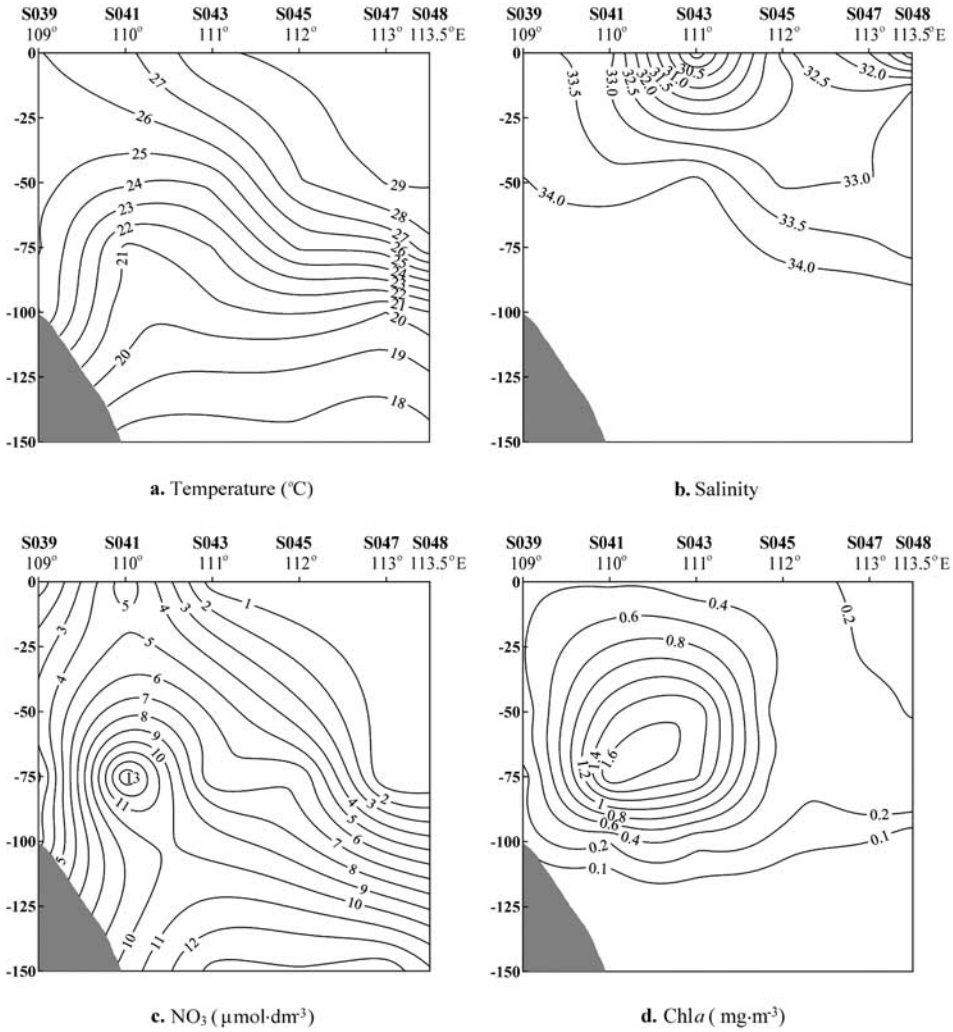

Figure 13. Similar to Figure 11, but for the transect between S039 and S048, showing the upwelling north of the Sunda shelf and the SCM underneath the Mekong River plume between S041 and S043.

Wu et al. [2003] reported that dissolved inorganic phosphorus (DIP) concentrations in the oligotrophic surface waters of the SCS decreased from ~0.02 μmol dm^{-3} in March 2000 to ~0.005 μmol dm^{-3} in July 2000. Therefore N:P was still higher than the Redfield ratio in summer. *Cai et al.* [2002] documented vertical fluxes of nitrate and phosphate to the euphotic zone yielding a N/P molar ratio of 35, which was significantly higher than the Redfield ratio and revealed P-limitation in the upper 300 m of the water column in the SCS. The low phosphorus concentration probably resulted from phytoplankton consumption and less supplementation from deep water because of the strong thermocline. As a response to the phosphorus depletion in the eastern and southern regions of the SCS (Figure 3b), the dominant species in phytoplankton communities shifted from diatoms to dinoflagellates and cyanophytes, which resulted in a high abundance of non-diatom species in the phytoplankton communities in these regions (Figure 6a).

6. Conclusions

[48] The present large-scale multidiscipline survey revealed clearly coupled physical-chemical-biological oceanographic processes in relation to phytoplankton stocks and production in the study area. Along the

Table 6. Correlations (r) Between Chl *a* and the Related Parameters in the Major Mesoscale Eddies in the SCS in 1998[a]

	Temperature		Salinity		NO_3		PO_4		SiO_3		DO		
Season	r	p	r	p	r	p	r	p	r	p	r	p	n
Summer	−0.83	<0.01	0.79	<0.01	0.68	<0.01	0.68	<0.01	0.68	<0.01	−0.63	<0.01	20
Winter	−0.69	<0.01	0.72	<0.01	0.76	<0.01	0.75	<0.01	0.80	<0.01	−0.64	<0.05	12

[a]Here (1-p)% defines the correlation significance level.

western, northwestern, and northern coasts and shelf of the SCS, the summer monsoon drives a northeastward current and induces upwelling through Ekman transport. The upwelling regions indicated by areas of low temperature, high salinity, rich nutrients, low DO concentration, and high Chl *a* and primary production were mainly found in the central basin off Vietnam, southeast of Hainan Island, and north of the Sunda Shelf during the southwest monsoon prevailing in summer. In winter, upwelling induced by mesoscale features, northwest of Luzon, the basin area off Vietnam, and the Sunda Shelf break, produced a strong cold trough oriented from the southwest to the northeast of the SCS. A high subsurface Chl *a* maximum was found, which can be attributed to the photosynthetic picoplankton, the most important contributor to biomass and production of the phytoplankton communities in both summer and winter in the SCS. Phosphorus depletion at the surface during summer resulted in a succession of phytoplankton species.

[49] In this paper, the seasonal distributions of phytoplankton in the SCS have been depicted and their link to the coupled physical-chemical-biological oceanographic processes has been identified. However, studies on the same topics during the monsoon transition seasons, i.e., spring and autumn, are needed in the future to understand the complete climatological succession and annual cycle. Furthermore, more extensive studies on physical-biological coupling within the mesoscale cold eddies and warm pools using both shipboard measurements and satellite remote sensing as well as time series observations are also needed.

[50] **Acknowledgments.** We thank the National Science Foundation of China (NSFC) for funding this study (grants 49776309, 40176035, and 90211021), and the Department of Science and Technology, SOA, China, for the opportunity to participate in the multidisciplinary cruises. We also wish to express our thanks to J. Xu and the Department of Marine Chemistry, SIO, for sharing their hydrological and chemical data with us, and to M. Shi for significant discussions on hydrodynamic features of the SCS. We thank Paul Harrison and the two anonymous reviewers for their comments and suggestions.

References

Allen, C. B., J. Kanda, and E. A. Laws (1996), New production and photosynthetic rates within and outside a cyclonic mesoscale eddy in the North Pacific subtropical gyre, *Deep Sea Res., Part I*, *43*, 917–936.

Cai, P., J. Huang, M. Chen, L. Guo, G. Liu, and Y. Qiu (2002), New production based on ^{228}Ra-derived nutrient budgets and thorium-estimated POC export at the intercalibration station in the South China Sea, *Deep Sea Res., Part I*, *49*, 53–66.

Chai, F., H. Xue, and M. Shi (2001a), Formation and distribution of upwelling and downwelling in the South China Sea, in *Oceanography in China*, vol. 13, edited by H. Xue, F. Chai, and J. Xu, pp. 117–128, China Ocean, Beijing.

Chai, F., H. Xue, and M. Shi (2001b), Upwelling east of Hainan Island, in *Oceanography in China*, vol. 13, edited by H. Xue, F. Chai, and J. Xu, pp. 129–137, China Ocean, Beijing.

Chai, F., H. Xue, and M. Shi (2001c), Hydrographic characteristics and seasonal variation of three anticyclonic eddies on the northern continental shelf of the South China Sea, in *Oceanography in China*, vol. 13, edited by H. Xue, F. Chai, and J. Xu, pp. 105–116, China Ocean, Beijing.

Chao, S. Y., P. T. Shaw, and S. Y. Wu (1996), Deep water ventilation in the South China Sea, *Deep Sea Res., Part I*, *43*, 445–466.

Chen, C., S. Wang, B. Wang, and S. Pai (2001), Nutrient budgets for the South China Sea basin, *Mar. Chem.*, *75*, 281–300.

Chen, X., Q. Chen, and L. Zhuang (1989), Distribution of chlorophyll *a* and photosynthesis, and the relations with the environmental factors in the central South China Sea, *Acta Oceanol. Sin.*, *11*, 349–355.

Chu, P. S., S. Lu, and Y. Chen (1997), Temporal and spatial variability of the South China Sea surface temperature anomaly, *J. Geophys. Res.*, *102*, 20,937–20,955.

Csanady, G. T., and P. Hamilton (1988), Circulation of slope water, *Cont. Shelf Res.*, *8*, 565–624.

Evans, C. A., J. E. O. Reilly, and J. P. Thomas (1987), *A Handbook for the Measurement of Chlorophyll a and Primary Production*, *BIOMASS Sci. Ser.*, vol. 8, edited by C. A. Evans, J. E. O'Reilly, and J. P. Thomas, 114 pp., Texas A&M Univ., College Station, Tex.

Falkowski, P. G., D. Ziemann, D. Kolber, and P. K. Bienfang (1991), Role of eddy pumping in enhancing primary production in the ocean, *Nature*, *352*, 55–58.

Fang, G., W. Fang, Y. Fang, and K. Wang (1998), A survey of studies on the South China Sea upper ocean circulation, *Acta Oceanogr. Taiwan.*, *37*, 1–16.

Goericke, R., and D. J. Repeta (1993), Chlorophylls *a* and *b* and divinyl chlorophylls a and b in the open subtropical North Atlantic Ocean, *Mar. Ecol. Prog. Ser.*, *101*, 307–313.

Gong, G. C., K. K. Liu, C. T. Liu, and S. C. Pai (1992), Chemical hydrography of the South China Sea and a comparison with the West Philippine Sea, *Terr. Atmos. Oceanic Sci.*, *3*, 587–602.

Gong, G. C., F. K. Shiah, K. K. Liu, Y. H. Wen, and M. H. Liang (2000), Spatial and temporal variation of chlorophyll *a*, primary productivity and chemical hydrography in the southern East China Sea, *Cont. Shelf Res.*, *20*, 411–436.

Guan, B. (1998), A review on studies of the South China Sea Warm Current, *Oceanol. Limnol. Sin.*, *29*, 322–327.

Han, W., H. Lin, and Y. Cai (1998), Study on the carbon flux of the South China Sea, *Acta Oceanol. Sin.*, *19*, 50–54.

Holm-Hansen, O., C. J. Lorenzen, R. W. Holms, and J. D. H. Strickland (1965), Fluorometric determination of chlorophyll, *J. Cons. Perm. Int. Explor. Mer.*, *30*, 3–15.

Huang, L. (1988), Distribution characteristics of chlorophyll *a* and estimation of primary productivity in the waters around Nansha Islands, in *Proceedings on Marine Biology of the South China Sea*, edited by X. Li and B. Morton, pp. 261–275, China Ocean, Beijing.

Huang, L. (1991), A preliminary study on the distribution of photosynthetic pigments and primary production in the sea area of Nansha Islands, in *Collected Papers on Marine Biology Study of Nansha Islands and the Adjacent Sea Areas (II)*, edited by Q. Chen, pp. 34–47, China Ocean, Beijing.

Huang, L., and C. Chen (1997), Distribution of chlorophyll *a* and primary productivity of Nansha Islands sea area in winter, in *A Study on Ecological Processes of Nansha Islands Sea Area* (I), edited by Q. Chen and L. Huang, pp. 1–15, Sci. Press, Beijing.

Hung, T., and C. C. H. Tsai (1972), Study on photosynthetic pigments and chemical nutrients in South China Sea, *Acta Oceanogr. Taiwan.*, *2*, 83–92.

Kuo, N. J., Q. Zheng, and C. R. Ho (2000), Satellite observation of upwelling along the western coast of the South China Sea, *Remote Sens. Environ.*, *74*, 463–470.

Liu, K. K., S. Y. Chao, P. T. Shaw, G. C. Gong, C. C. Chen, and T. Y. Tang (2002), Monsoon-forced chlorophyll distribution and primary production in the South China Sea: Observations and a numerical study, *Deep Sea Res., Part I*, *49*, 1387–1412.

Liu, X., and Ch. Liu (1984), Distribution of chlorophyll a in the sea areas nearby Xisha and Zhongsha Islands, *Coll. Pap. Mar. Sci.*, *5*, 63–66.

Liu, Z., Y. Cai, and X. Ning (1998), Distribution characteristics of size-fractionated chlorophyll a and primary productivity in Beibu Gulf, *Acta Oceanol. Sin.*, *17*, 71–83.

Liu, Z., J. Xu, L. Li, and M. Shi (2001), Characteristics and distribution of water masses in the South China Sea during summer and winter of 1998, in *Oceanography in China*, edited by H. Xue, F. Chai, and J. Xu, pp. 221–230, China Ocean, Beijing.

McGillicuddy, D. J., Jr., A. R. Robinson, D. A. Siegel, H. W. Jannasch, R. Johnson, T. D. Dickey, J. McNeil, A. F. Michaels, and A. H. Knap (1998), Influence of mesoscale eddies on new production in the Sargasso Sea, *Nature*, *393*, 263–265.

Metzger, E. J., and H. E. Hurlburt (1996), Coupled dynamics of the South China Sea, the Sulu Sea and the Pacific Ocean, *J. Geophys. Res.*, *101*, 12,331–12,352.

Morimoto, A., K. Yoshimoto, and T. Yanagi (2000), Characteristics of sea surface circulation and eddy field in the South China Sea revealed by satellite altimetric data, *J. Oceanogr.*, *56*, 331–344.

Ning, X., and Z. Liu (1988), The patterns of distribution of chlorophyll *a* and primary production in coastal upwelling area off Zhejiang, *Acta Oceanol. Sin.*, *7*, 126–136.

Ning, X., D. Vaulot, Z. Liu, and Z. Liu (1988), Standing stock and production of phytoplankton in the estuary of the Changjiang (Yangtze River) and the adjacent East China Sea, *Mar. Ecol. Prog. Ser.*, *49*, 141–150.

Ning, X., Y. Cai, W. K. W. Li, and J. Shi (2003), Photosynthetic picoplankton in the northern South China Sea, *Acta Oceanol. Sin.*, *25*, 83–97.

Nishimoto, M. M., and L. Washburn (2002), Patterns of coastal eddy circulation and abundance of pelagic juvenile fish in the Santa Barbara Cannel, California, USA, *Mar. Ecol. Prog. Ser.*, *241*, 183–199.

Nitani, H. (1972), Beginning of the Kuroshio, in *Kuroshio*, edited by H. Stommel and K. Yoshida, pp. 129–163, Univ. of Wash. Press, Seattle.

Olaizola, M., D. A. Ziemann, P. K. Bienfang, W. A. Walsh, and L. D. Conquest (1993), Eddy-induced oscillations of the pycnocline affect the floristic composition and depth distribution of phytoplankton in the subtropical Pacific, *Mar. Biol.*, *116*, 533–542.

Rong, Z. (1994), The characteristics of surface circulation of the South China Sea during winter, *Mar. Forecasts*, *11*, 47–51.

Sadler, J. C., M. A. Lander, and L. K. Oda (1985), *Tropical Marine Climate Atlas*, vol. 1, *Indian Ocean and Atlantic Ocean*, Univ. of Hawaii, Honolulu.

San Diego-McGlone, M. L., G. S. Jacinto, V. C. Dupra, I. S. Narcise, D. O. Padayao, and I. B. Velasquez (1999), A comparison of nutrient characteristics and primary productivity in the Sulu Sea and South China Sea, *Acta Oceanogr. Taiwan.*, *37*, 219–229.

Seki, M. P., J. J. Polovina, R. E. Brainard, R. R. Bidigare, C. L. Leonard, and D. G. Foley (2001), Biological enhancement at cyclonic eddies tracked with GOES thermal imagery in Hawaiian waters, *Geophys. Res. Lett.*, *28*, 1583–1586.

Shaw, P. T. (1991), The seasonal variation of the intrusion of the Philippine Sea water into the South China Sea, *J. Geophys. Res.*, *96*, 821–827.

Shaw, P. T., and S. Y. Chao (1994), Surface circulation in the South China Sea, *Deep Sea Res.*, *41*, 1663–1683.

Shaw, P. T., S. U. Chao, K. K. Liu, S. C. Pai, and C. T. Liu (1996), Winter upwelling off Luzon in the northeast South China Sea, *J. Geophys. Res.*, *101*, 16,435–16,448.

Sournia, A. (1978), *Phytoplankton Manual*, 337 pp., U.N. Educ., Sci., and Cultural Org., Paris.

Steemann Nielson, E. (1952), The use of radioactive carbon (^{14}C) for measuring organic production in the sea, *J. Cons. Int. Explor. Mer.*, *18*, 117–140.

Strickland, J. D. H., and T. R. Parsons (1972), A practical handbook of seawater analysis, *Bull. Fish. Res. Board Can.*, *167*, 1–310.

Su, J., J. Xu, S. Cai, and O. Wang (1999), Circulation and eddies of the South China Sea, in *The Eruption and Evolution of Monsoon and its Interaction With Oceans in the South China Sea*, edited by Y. Ding and C. Li, pp. 66–72, Meteorol. Press, Beijing.

Takahashi, M., and T. Hori (1984), Abundance of picophytoplankton in the subsurface chlorophyll maximum layer in subtropical and tropical waters, *Mar. Biol.*, *79*, 177–186.

Tao, S. (1978), The monsoon of the Eastern Asia, in *Climatology Knowledge*, edited by Atmospheric Physics Institute, Academy Sinica, pp. 115–134, Sci. Press, Beijing.

Udarbe-Walker, M. J. B., and C. L. Villanoy (2001), Structure of potential upwelling areas in the Philippines, *Deep Sea Res.*, *Part I*, *48*, 1499–1518.

U.S. Naval Oceanographic Office (1969), *Bathymetric Atlas of the Northwestern Pacific Ocean*, *Publ. 1301*, NAVOCEANO, Washington, D. C.

Vaillancourt, R. D., J. Marra, M. P. Seki, M. L. Parsons, and R. R. Bidigare (2003), Impact of a cyclonic eddy on phytoplankton community structure and photosynthetic competency in the subtropical North Pacific Ocean, *Deep Sea Res.*, *Part I*, *50*, 829–847.

Wang, L., C. J. Koblinsky, J. Chester, and S. Howden (1999), Mesoscale variability in the South China Sea from the TOPEX/Poseidon altimetry data, *Deep Sea Res.*, *Part I*, *47*, 681–708.

Williams, R. G., and M. J. Follows (2003), Physical transport of nutrients and the maintenance of biological production, in *Ocean Biogeochemistry*, edited by M. J. R. Fasham, chap. 2, pp. 19–51, Springer-Verlag, New York.

Wu, J., S. W. Chung, L. S. Wen, and K. K. Liu (2003), Dissolved inorganic phosphorus, dissolved iron, and *Trichodesmium* in the oligotrophic South China Sea, *Global Biogeochem. Cycles*, *17*, 1008, doi:10.1029/2002GB001924.

Wyrtki, K. (1961), Physical oceanography of the Southeast Asian waters, in *Scientific Results of Marine Investigations of the South China Sea and the Gulf of Thailand*, *NAGA Rep.*, vol. 2, pp. 1–195, Scripps Inst. of Oceanogr., La Jolla, Calif.

Xu, J., H. Xue, M. Shi, and Z. Liu (2001), Observation and study of the circulation and meso-scale eddies in the upper layer of the South China Sea in summer of 1998, in *Oceanography in China*, vol. 13, edited by H. Xue, F. Chai, and J. Xu, pp. 178–187, China Ocean, Beijing.

Xue, H., F. Chai, D. Xu, and M. Shi (2001a), Characteristics and seasonal variation of the coastal currents in the South China Sea, in *Oceanography in China*, vol. 13, edited by H. Xue, F. Chai, and J. Xu, pp. 64–75, China Ocean, Beijing.

Xue, H., F. Chai, D. Xu, and M. Shi (2001b), A circulation model of the South China Sea, in *Oceanography in China*, vol. 13, edited by H. Xue, F. Chai, and J. Xu, pp. 1–14, China Ocean, Beijing.

Xue, H., F. Chai, N. R. Pettigrew, D. Xu, M. Shi, and J. Xu (2004), Kuroshio intrusion and the circulation in the South China Sea, *J. Geophys. Res.*, *109*, C02017, doi:10.1029/2002JC001724.

Yin, K. (2002), Monsoonal influence on seasonal variations in nutrients and phytoplankton biomass in coastal waters of Hong Kong in the vicinity of the Pearl River estuary, *Mar. Ecol. Prog. Ser.*, *245*, 111–122.

Zeng, Q., R. Li, and Z. Ji (1989), The computation of monthly average current, *Atmos. Sci.*, *13*, 127–138.

Y. Cai, C. Liu, X. Ning, and J. Shi, Second Institute of Oceanography, State Oceanic Administration, 36 Baochubei Road, Hangzhou, Zhejiang 310012, China. (ning@sio.zj.edu.cn)

F. Chai and H. Xue, School of Marine Sciences, 5741 Libby Hall, University of Maine, Orono, ME 04469-5741, USA. (fchai@maine.edu)